A concept of homeomorphic defect for defining mostly conjugate dynamical systems

Joseph D. Skufca[a] and Erik M. Bollt[b]
Department of Mathematics, Clarkson University, Potsdam, New York 13699-5815, USA

(Received 11 September 2007; accepted 27 December 2007; published online 11 March 2008)

A centerpiece of dynamical systems is comparison by an equivalence relationship called topological conjugacy. We present details of how a method to produce conjugacy functions based on a functional fixed point iteration scheme can be generalized to compare dynamical systems that are not conjugate. When applied to nonconjugate dynamical systems, we show that the fixed-point iteration scheme still has a limit point, which is a function we now call a "commuter"—a nonhomeomorphic change of coordinates translating between dissimilar systems. This translation is natural to the concepts of dynamical systems in that it matches the systems within the language of their orbit structures, meaning that orbits must be matched to orbits by some commuter function. We introduce methods to compare nonequivalent systems by quantifying how much the commuter function fails to be a homeomorphism, an approach that gives more respect to the dynamics than the traditional comparisons based on normed linear spaces, such as L^2. Our discussion addresses a fundamental issue—how does one make principled statements of the degree to which a "toy model" might be representative of a more complicated system? © *2008 American Institute of Physics*.
[DOI: 10.1063/1.2837397]

A primary interest of this work will be to develop principles and methods to compare dynamical systems when they are *not* necessarily equivalent (in the sense of conjugacy), but in a manner that respects the behavioral implications of conjugacy. That is, we extend a centerpiece notion in dynamical systems whose equivalence relationship called topological conjugacy can either judge two systems as the same, or not the same, a boolean answer. To this end, we detail methods to produce conjugacy functions based on a functional fixed-point iteration scheme. We then show how this same fixed-point iteration can be generalized to compare dynamical systems that are not conjugate. When applied to nonconjugate dynamical systems, we show that the fixed-point iteration scheme still has a limit point, which is a function we now call a "commuter"—a nonhomeomorphic change of coordinates translating between dissimilar systems. This translation is natural to the concepts of dynamical systems in that it matches the systems within the language of their orbit structures, meaning, in some sense, that orbits must be matched to orbits by some commuter function. We introduce methods to compare nonequivalent systems by quantifying how much the commuter function fails to be a homeomorphism, an approach that gives more respect to the dynamics than the traditional comparisons based on normed linear spaces, such as L^2. We coin the phrase "defect," between two systems embedded in measure spaces, to describe relative measured failures of the commuter to be a homeomorphism. Our discussion addresses a fundamental issue—how does one make principled statements of the degree to which a "toy model" might be representative of a more complicated system.

I. INTRODUCTION

The complex oscillations we see in the physical world around us have been a subject of intense study in practically every branch of science and engineering, as documented in many textbooks,[1] review articles,[2] and popular literature.[3] Since the beginnings of the field of dynamical systems by Henri Poincaré,[4] characterizing a dynamical system has focused on examining the topological and geometric features of orbits, rather than focusing on the empirical details of the solution of the dynamical system with respect to a specific coordinate system. One seeks to understand coordinate-independent properties, such as the periodic orbit structure, the count, and stability of periodic orbits. The question of whether two systems are dynamically the same has evolved into the modern notion of deciding if there is a conjugacy between them.[5–9]

Since modeling is fundamental in science, we may ask, "What do we mean by a model?" We would answer that a model of the "true" system (physical perhaps) is a simpler system [perhaps of ordinary differential equations (ODEs), for example] that is "descriptive" of some aspects of the original system. A model should be a system that is somehow easier to analyze. Although the model is only *representative* of the true system, it might have been constructed with first principles in mind and may teach us about the mechanisms of the true system. Given these notions, we tend to speak of a "toy model"—a dynamical system that is much "like" the "real" system. These subjective evaluations are assertions that the model is *satisfactory*, but fail to distinguish excellent

[a]Electronic mail: jskufca@clarkson.edu.
[b]Electronic mail: ebollt@clarkson.edu.

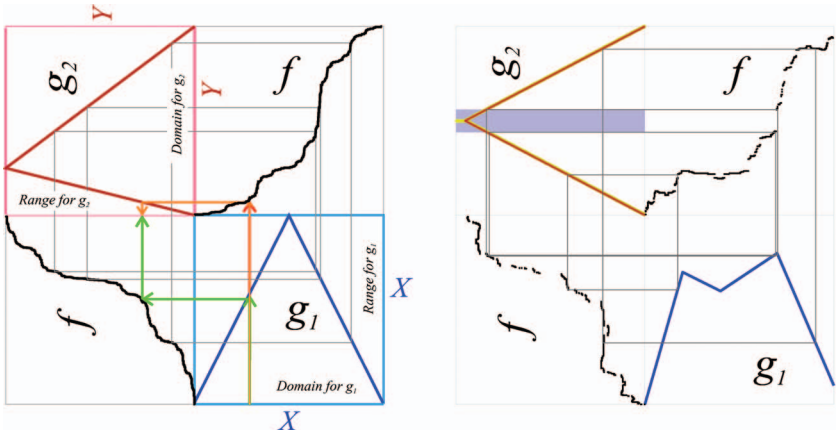

FIG. 1. (Color) Conjugacy and commuter, shown as quadwebs. (Left) Quadwebs allow visualization of the commutative relationship of Eq. (1). The lower right panel shows a symmetric full shift tent map, g_1 acting on space $X=[0,1]$. The upper right panel shows a graph of the conjugacy function, f, which maps $X=[0,1]$ on the horizontal to $Y=[0,1]$ on the vertical. The upper left panel shows a skew tent map g_2 acting on $Y=[0,1]$, where we have oriented the graph by rotating the figure counterclockwise so that $y=f(x)$ lies in the domain of this graph. Similarly, the lower left is another copy of f, oriented to allow points x in the range of g_1 to map to points y in the range of g_2. The rectangles illustrate that the maps actually satisfy Eq. (1), $f\circ g_1=g_2\circ f$. In this example, the conjugacy is strictly increasing, yet its derivative is 0 almost everywhere, a Lebesgue singular function. In Appendix B, we discuss this *singular* property. (Right) The two maps shown are obviously not conjugate, as there are a different number of humps; g_1 requires a subshift of 2-symbols Σ_2', and g_2 requires a subshift Σ_4' of 4-symbols. So any f that satisfies Eq. (1) cannot be a homeomorphism. The "solution" f, found by fixed point iteration, we call a "commuter," since it solves $f\circ g_1=g_2\circ f$. We see that as a function $f:[0,1]\to[0,1]$, the commuter fails each of the properties of continuity, one-one-ness, onto-ness, and f^{-1} fails to exist at certain points (apparently a Cantor set). See Appendix A for further description of Quadwebs.

models from mediocre ones. For this reason, we assert that *quantifying the quality* of a model is an essential problem in science. A primary interest of this work will be to develop principles and methods to compare dynamical systems when they are *not* necessarily equivalent (in the sense of conjugacy), but in a manner that respects the behavioral implications of conjugacy.

A standard approach to quantifying model accuracy is to measure how "close" the model is to the original system, where "close" depends on what aspects of the system we are trying to model. In many cases, *prediction* is our modeling goal, such as when forecasting the weather. The quality of prediction is grounded in standard numerical analysis on Banach spaces: the "goodness" of short-term predictions is based on measurement of residual error. However, in *dynamical systems*, a model's quality is typically *not* based on such error analysis. Continuing, for the sake of example, in the field of meteorology, we cite a famous historical example to highlight this long recognized issue. Consider Lorenz's 1965 paper about his 28-variable ODE model of the weather.[10] The model consists of Galerkin's projection of a two-level geostrophic model for fluid flow in the atmosphere. About the matter of choice of parameter values that are initially free in the model, the tuning of which led to dramatically different dynamic behavior due to a plethora of possible bifurcations, Lorenz says, "Our first choice of constants lead to periodic variations. Subsequent choices yielded irregular…." He relied on his expert knowledge as a meteorologist concerning what "reminded" him of oscillations of realistic weather. Even by the time of his 1998 paper on a 40-variable model,[11] we quote, "Regardless of how well or how poorly the equation of the model resemble those of the atmosphere, it is essential to know, before proceeding with our experiments, how closely the model resembles the atmosphere in its behavior." Therefore, we summarize that even today, as this central step of modeling moves across the sciences, we in the applied dynamical systems community still tend to choose the "best model" from a model class in an intuitive manner. Our research here intends to address this issue of *quantifying the quality* in a mathematically grounded manner.

A. Comparing dynamical systems: On conjugacy and nonhomeomorphic commuters

Given two dynamical systems, $g_1:X\to X$, and $g_2:Y\to Y$, the fundamental departure from a typical measurement of approximation between the two dynamical systems is that we do not directly compare g_1 and g_2 under an embedding in a Banach space (e.g., measuring, say, $\|g_1-g_2\|_{L^2}$) because such measurements pay no regard to the central equivalence relationship in dynamical systems, namely conjugacy. Two systems are conjugate if there is a homeomorphism $h:X\to Y$ between the underlying phase space (h must be 1-1, onto, continuous, and h^{-1} must be continuous), and h must commute the mappings at each point $x\in X$. This is not only the fundamental equivalence relationship of the field, it reflects the practical notion that h is an "exact" change of coordinates so that the mappings behave exactly the same in either coordinate system. See in Fig. 1 our new quadweb representation of a commuter and Appendix A for further description.

We give the name "commuter" to any function $f:X\to Y$ that satisfies the commuting relationship,

$$f\circ g_1=g_2\circ f, \tag{1}$$

and note that a commuter will be a conjugacy only if it is a homeomorphism. The commuter provides a matching between trajectories for g_1 and g_2; over- and/or under-representations are reflected as 1-1 and onto problems in f, while trajectories that permit matching only for finite time

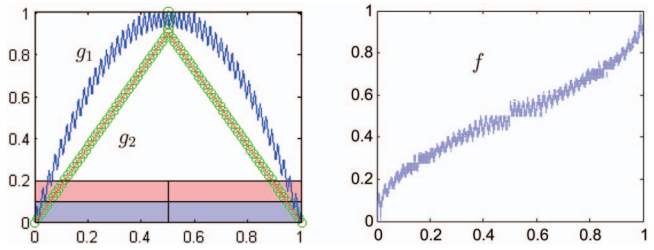

FIG. 2. (Color) Modeling a noisy logistic map. (Left) A "noisy" logistic map g_1 (blue) is obviously near the full logistic map $4x(1-x)$, in both any $L^p([0,1])$, $p \geq 1$, as well as in the sup-norm, but not in the $C^1([0,1])$ norm, as the map was constructed with slope $|g_1'(x)|=10$ everywhere that it exists. The green circles graph a tent map g_2 (with vertical extension) which is our "best" model within the family of symmetric tent maps. (Right) The resulting commuter f between g_1 and this tent map g_2 is reminiscent of the homeomorphism $h(x)=1/2[1-\cos(\pi x)]$ between the full logistic map and the full tent map. Whereas h is a diffeomorphism, f is not even a homeomorphism, though our visual impression is that we would not need to move the points (on the graph of f) very far to achieve a homeomorphism.

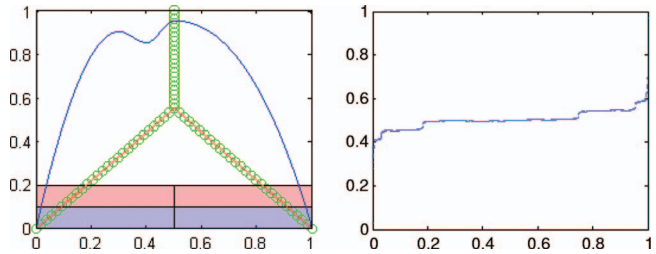

FIG. 3. (Color) (Left) Logistic map with "just a little" extra dynamics. These maps are not as far from conjugacy as appearances might indicate, and they are obviously not close in any L^p or C^r norm. That g_1 has two humps, and g_2 has one hump, which suggests that subshifts of Σ_4 and Σ_2, respectively, are required to represent the dynamics. In fact, g_1 behaves as if it is almost conjugate to a trapezoid map (Ref. 37), also known as a gap-map (Ref. 38), since it does not take a large perturbation to replace the extra humps of $x \in (0.25, 0.5)$, with a horizontal line segment. (Right) Note the nonmonotonicity in the commuter, indicating that g_1 has dynamics that are not matched by g_2. In the sense of defect, the tent map shown is the best dynamical match to the blue map; even though we can see clearly that there are closer tent maps in an L^2 sense, they are not dynamically closer.

are related to discontinuities in f. Our fundamental approach is that we suggest to develop measures of commuters f to quantify "how much" the f may fail to be a homeomorphism. Such measures quantify the dissimilarity of g_1 and g_2 in a manner that respects the fundamental philosophy of dynamical systems.

B. Examples of commuters of "close" dynamical systems

Our primary interest is in comparing dynamical systems with methods that respect the notion of conjugacy. We will use the commuter to indicate how well the systems are matched (from a dynamical perspective) by observing the deviation from homeomorphism. These examples are indicative goal problems, selected to allow for a clear presentation in the one-dimensional setting. The eventual goal of our work will be to extend this approach to compare multivariate systems, including diffeomorphisms and flows. Although the examples and constructions of this paper focuses on one-dimensional examples, the measure theoretic definitions of defect are meant to generalize naturally.

Example Problem: Modeling a noisy logistic map. It is well known that the logistic map $g_1(x)=rx(1-x)$ is conjugate to the tent map $g_2(x)=a(1-2|x-1/2|)$ for parameter values $r=4$ and $a=2$. The conjugacy $h(x)=1/2[1-\cos(\pi x)]$ provides perhaps the most studied example in the pedagogy of dynamical systems for teaching conjugacy. If r is perturbed even slightly, the maps fails to be a conjugate. Now consider a system with a much stronger perturbation, like a noisy version of the logistic map, which is obviously not conjugate to the tent map. The commuter shown in Fig. 2 (right) is not a homeomorphism, since it fails at least one-one-ness, which we see immediately upon inspection. The commuter gives the orbit equivalence between the two maps and is the key to understanding the quality of a model. One could argue that the tent map shown is a good candidate to model this "noisy logistic map" because although it simplifies the small-scale dynamics, it captures the main features of the large-scale orbit structure. We quantify this argument by measuring the defect of f using techniques described in Sec. V.

Example Problem: Logistic map with "just a little" extra dynamics. In Fig. 3, we see a map with two humps, which is clearly not conjugate to any one hump map such as the tent map. However, in some sense, the dynamics are "mostly" very similar to those of the tent map. Inspection of the orbit equivalence through the commuter function in Fig. 3 (right) clearly shows the failure of f to be a homeomorphism due to the failure of all four of the properties of continuity both ways, one-one-ness, and onto-ness. In a measured sense that we call "homeomorphic defect" defined in Sec. V, the failure is not large. We will conclude that a large fraction of the dynamics of g_1 "mostly" match most of the dynamics of g_2, suggesting that the model with one hump is reasonable. More details of this example are in the figure caption to Fig. 3.

C. Some background

In the above examples, the "models" (g_2's) were chosen such that the commuter had a small homeomorphic defect. An alternative, traditional method is to consider relative entropies between the systems. For the noisy logistic map in Fig. 2 (which is semiconjugate to a shift map embedded in a symbol space of many symbols), selecting a model to minimize the entropy difference would mean that we would choose a very steep and high tent map. In an experimental situation, depending on our ability to resolve the spatial fine scales of the thin humps, the noisy map will appear more like the original logistic map of $h_T=\ln(2)$ than like a map of higher entropy, and we might prefer that a simplifying model should reflect this lower entropy. We sometimes refer to well-modeled systems as being "almost conjugate." There is a notion of almost conjugacy already in the symbolic dynamics literature,[7,12] through "orbit equivalence," used to compare two shift spaces, which relies on the existence of a factor map between the two shift spaces. Although the term "defect" has been used to describe the degree to which such a factor map fails to be injective,[13] we define *homeomorphic defect* using an entirely different construct for use in a very different setting—where systems are not equivalent. Ergodic

theory provides other metrics on equivalence classes of dynamical systems, based on notions such as Kakutani equivalence or metric isomorphism.[14] Our work is complementary to that work, but it is somewhat different in that we can directly compare two maps (even when they are not shift maps) and explicitly construct the commuter function—the realization of the factor map. Our goal is to provide a measure between equivalence classes based on *topological conjugacy*. Quantifying the similarity between two dynamical systems directly through measuring a change of coordinates between them is a departure from general literature, and the only paper we find remotely in the same vein is that of Yuan–Yorke *et al.*,[15] whereas the methods and scope were quite different. We believe the idea is natural and general.

II. ON CONSTRUCTION OF COMMUTERS

In this section, we use the tent map as an easy setting to introduce how the commuter, or would be conjugacy, can be explicitly constructed by a fixed-point iteration scheme. In this simple setting, we will rigorously prove several aspects of the existence and convergence of the fixed-point iteration. In subsequent sections, we will see that for more complicated problems, the methods seem to work numerically well beyond our sufficient theorems. In subsequent sections, we will introduce the commuter's role in measuring homeomorphic defect.

While here we propose to use commuters between dynamical systems in a unique way as part of developing our defect measure, for the construction step, we should point to the line of work dating to Schub in 1969,[16] and further studied, for example, in Ref. 17 and reviewed in the popular textbook by de Melo and van Strien.[18] These are related to our Lemmas 1–3. In particular, see Theorem II 2.1 in Ref. 18. Therein, endomorphisms, including general conjugacies, are constructed using methods based on the contraction mapping principle related to what we describe in Sec. II. Generalization for the multivariate expanding case can be found in Ref. 16. A major difference between our work and that of Shub is our interest in comparing arbitrary domains between the maps, which has required that we develop an extended inverse $\hat{g}_{2i}^{-1}$ in Eq. (30) when defining our contraction operators, $\mathfrak{C}_{g_1}^{g_2}$.

A. A conjugacy between tent maps

Consider the family of skew tent maps $S(x)$ defined on $[0, 1]$, with the following restrictions:

- $S(0)=0$ and $S(1)=0$.
- The peak of the tent occurs at $S(\alpha)=\beta$, with $0<\alpha<1$.
- To ensure that the map is locally expanding, we require

$$\max(\alpha, 1-\alpha) < \beta \leqslant 1. \tag{2}$$

Define this family $\mathcal{S}$, where the family is parametrized by α and β, the coordinates of the peak of the tent. Denote a specific member of this family as $S_{\alpha,\beta}$, where the coordinates of the peak of that tent are at (α,β). Within this family of skew tents, consider the subset of maps that are symmetric about $x=1/2$. We denote this subfamily as $\mathcal{T}$, where $\mathcal{T}\subset\mathcal{S}$. An arbitrary member $T_\nu\in\mathcal{T}$ is defined by $T_\nu := S_{1/2,\nu}$.

First, we note the following lemma regarding the existence of a conjugacy:

Lemma 1. *Let $S_{a,b}$ be a particular member of $\mathcal{S}$. Then there exists a ν_0 such that $S_{a,b}$ is conjugate to $T_{\nu_0}\in\mathcal{T}$.*

Sketch of Proof: Kneading sequences need to be matched, and we know that there is a value of ν_0 that matches the kneading sequences and hence symbolic dynamics by a so-called intermediate value theorem of kneading sequences, which can be found in either Misiurewicz and Visinescu[20] or Collet and Eckmann.[21] Although matching symbolic dynamics is not enough to prove that the maps are conjugate, it is necessary. Similarly, the fact that both maps are strictly monotone is enough to guarantee that monotone laps map to monotone laps, from which it can be shown that there is a match between any two points with the same symbolic itineraries. The match of symbolic dynamics does guarantee a match between the eventually periodic points. Because both maps are assumed to be everywhere expanding, the matching can be extended to the entire interval, with h and h^{-1} continuous. □

The remainder of this section is constructed under the presumption that we have chosen a particular value for a and b, and though they are arbitrary, they remain fixed. The map $S\equiv S_{a,b}$ will be used to symbolize this arbitrary but fixed map. To find the conjugacy whose existence is indicated by Lemma 1, we need to solve the functional equation

$$S\circ h(x) = h\circ T(x). \tag{3}$$

In particular, one must find an h that not only satisfies Eq. (3) but is also a homeomorphism. In general, there is no direct technique to find such an h. Instead, we propose an indirect solution approach: we create a fixed-point iteration scheme that converges to a solution. The rest of this section describes the development of that iterative scheme, which we decompose into three components:

- Creating a contraction mapping that generates solutions to the commutative diagram.
- Explaining why the result of that contraction yields a conjugacy h when S and T are conjugate (or, equivalently, when $\nu=\nu_0$, with ν_0 known).
- Describing an iterative technique to find ν_0 when a and b are given, but the required conjugacy parameter value (from Lemma 1) is not known.

B. A contraction mapping from the commutative relationship

On the interval $[0,1/2]$, the explicit form for the symmetric tent map is $T(x)=2\nu_0 x$. Substituting into Eq. (3) gives

$$S\circ h(x) = h(2\nu_0 x). \tag{4}$$

To write an explicit description of S, we note that the interval $[0,1/2]$ describes the domain of the left part of the tent map T. Because we are identifying the *conjugacy* between these two maps (which preserves the kneading sequence), we conclude that $h[0,1/2]=[0,a]$ because $[0,a]$ is the domain of

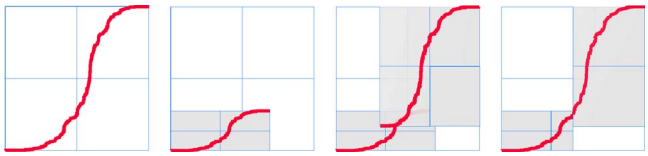

FIG. 4. (Color online) Satisfying the functional equation. Equation (7) can be viewed as a process: take $h(x)$ (panel 1) and make a copy, shrunken by a/b in the vertical and by $2\nu_0$ in the horizontal (panel 2). Take a second copy, scaled the same horizontally, but vertically scaled by $(1-a)/b$. Rotate this copy by 180 degrees and place it in the upper right portion of the unit square (panel 3). Then truncate the left copy to the interval $[0,1/2)$ and the right copy to $[1/2,1]$. The result (panel 4) should return the original $h(x)$.

the left part of the S map. On that interval, $S(u)=b/au$, and substitution into Eq. (4) gives

$$\frac{b}{a}h(x)=h(2\nu_0 x). \tag{5}$$

Similar logic applied to the interval $(1/2,1]$ gives

$$\frac{b}{1-a}(1-h(x))=h(2\nu_0(1-x)). \tag{6}$$

Therefore, the conjugacy function $h(x)$ must satisfy the functional equation,

$$h(x)=\begin{cases}\dfrac{a}{b}h(2\nu_0 x) & 0\leqslant x\leqslant 1/2\\[2ex] 1-\dfrac{1-a}{b}h(2\nu_0(1-x)) & 1/2<x\leqslant 1.\end{cases} \tag{7}$$

(see Fig 4 for a graphical representation of this relationship).

Since a conjugacy should map turning points to turning points, we note that

$$h(1/2)=a. \tag{8}$$

Additionally, evaluating Eq. (7) at $x=1/2$, we have

$$h(1/2)=a=\frac{a}{b}h(\nu_0), \tag{9}$$

yielding that

$$h(\nu_0)=b. \tag{10}$$

Using Eq. (7) as a guide, we now create an operator whose fixed point will satisfy the commutative diagram. We consider the space $B([0,1],\mathbb{R})$, the set of all bounded functions from [0, 1] to the real numbers, which is a Banach space, with norm given by

$$\|f\|\equiv\|f\|_\infty:=\sup_{x\in[0,1]}|f(x)|. \tag{11}$$

Then we form the closed subset $\mathcal{F}\subset B([0,1],\mathbb{R})$, defined by

$$\mathcal{F}=\{f|f:[0,1]\to[0,1]\}, \tag{12}$$

the set of functions from [0, 1] to [0, 1]. Then given (a,b) satisfying $\max(a,1-a)<b<1$, we define a one-parameter family of operators $M_\nu:\mathcal{F}\to\mathcal{F}$ for $1/2<\nu\leqslant 1$,

$$M_\nu f(x):=\begin{cases}\dfrac{a}{b}f(2\nu x) & 0\leqslant x\leqslant 1/2\\[2ex] 1-\dfrac{1-a}{b}f(2\nu(1-x)) & 1/2<x\leqslant 1.\end{cases} \tag{13}$$

The constraints on the parameters a,b and ν are required to ensure that $\mathcal{F}$ is mapped into itself, but they also cause the operator to be a contraction.

Lemma 2. *M_ν is a uniform contraction on $\mathcal{F}$, where the contraction is with respect to $\|\cdot\|_\infty$.*

Proof. Define

$$\lambda=\max\left(\frac{a}{b},\frac{1-a}{b}\right). \tag{14}$$

Then $0<\lambda<1$. We compute

$$\|M_\nu f_1-M_\nu f_2\|_\infty=\sup_x|M_\nu f_1(x)-M_\nu f_2(x)|. \tag{15}$$

We decompose this problem into the two cases $x\leqslant 1/2$ and $x>1/2$. For the first case,

$$\begin{aligned}&\sup_{0\leqslant x\leqslant 1/2}|M_\nu f_1(x)-M_\nu f_2(x)|\\&\quad=\sup_{0\leqslant x\leqslant 1/2}\left|\frac{a}{b}(f_1(2\nu x)-f_2(2\nu x))\right|\\&\quad\leqslant\frac{a}{b}\sup_{0\leqslant y\leqslant 1}|f_1(y)-f_2(y)|\leqslant\lambda\|f_1-f_2\|.\end{aligned}$$

Similarly

$$\begin{aligned}&\sup_{1/2<x\leqslant 1}|M_\nu f_1(x)-M_\nu f_2(x)|\\&\quad=\sup_{1/2<x\leqslant 1}\left|\frac{1-a}{b}(f_1(2\nu x)-f_2(2\nu x))\right|\\&\quad\leqslant\frac{1-a}{b}\sup_{0\leqslant y\leqslant 1}|f_1(y)-f_2(y)|\leqslant\lambda\|f_1-f_2\|.\end{aligned}$$

So M_ν is a contraction, with contraction constant λ. Because λ does not depend on ν, the contraction is *uniform*. □

With this groundwork in place, we establish the existence of a fixed point of the operator.

Lemma 3. *There is a unique $f_\nu\in\mathcal{F}$ satisfying*

$$M_\nu f_\nu=f_\nu. \tag{16}$$

Moreover, for an arbitrary $f_0\in\mathcal{F}$, if we define the sequence of functions

$$f_{n+1}=M_\nu f_n, \tag{17}$$

this sequence will converge to f_ν:

$$f_\nu:=\lim_{n\to\infty}f_n. \tag{18}$$

Proof. The lemma is a direct application of the Banach-Caccioppoli Contraction Mapping Principle,[22] and we simply need to verify that we satisfy the hypothesis of the theorem. Since $B([0,1],\mathbb{R})$ is a Banach space, with $\mathcal{F}$ a closed subset, and $M_\nu:\mathcal{F}\to\mathcal{F}$, the theorem applies, and the conclusions are immediate. □

Remark: For any chosen ν, by construction, the fixed

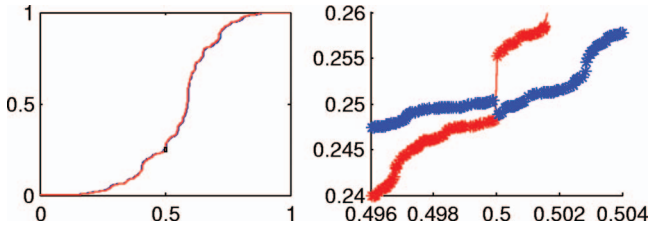

FIG. 5. (Color) Resolving ν_0. Fixing $a=0.25$ and $b=0.9$, we graph f_ν for $\nu=0.72$ (red) and $\nu=0.73$ (blue). The zoomed panel (right) illustrates that $\hat{\lambda}(0.72)<0$ (the red curve jumps up at $x=0.5$) while $\hat{\lambda}(0.73)>0$ (the blue curve jumps down).

point f_ν will satisfy the requirements of the commutative diagram, at least over some portion of its domain (see Appendix A for more detail). The question remains as to whether it is a conjugacy function between the two maps S and T_ν. If the two maps are conjugate, which we know is possible by Lemma 1 by choosing the parameter to be $\nu=\nu_0$, then it is straightforward to check that the f_{ν_0} produced by the fixed-point iteration scheme is that conjugacy function, and we call it $h(x)=f_{\nu_0}(x)$. It is important to note for much of the following development that even if the two maps S and T_ν are not conjugate and so no conjugacy function $h(x)$ exists, the fixed-point iteration still produces a function f_ν satisfying the commutative diagram. However, it cannot be a homeomorphism.

C. The search for ν_0: A problem of parameter estimation

Suppose we are given a chaotic map from the family $\mathcal{S}$. (In other words, (a,b) are fixed.) By Lemma 1, we know that there is a ν_0 such that map T_{ν_0} is conjugate to S. In this section, we give a short explanation of how we find that conjugate map.

When $\nu\neq\nu_0$, the maps $S_{a,b}$ and T_ν are not conjugate, and while the existence of f_ν as the fixed point of a contraction is guaranteed by Lemma 3, f_ν fails to be a homeomorphism. We find that for $\nu<\nu_0$, f_ν is monotone increasing, but not continuous and not onto $[0,1]$. The largest "gap" is at $x=1/2$. Because f_ν satisfies a recursive formulation (which creates a self-similar structure), a scaled version of this defect appears at all x coordinates associated with the kneading sequence of T. We define

$$\hat{\lambda}(\nu) := \lim_{x\to(1/2)^-} f_\nu(x) - a \tag{19}$$

as a way of measuring this "signed defect," with $\hat{\lambda}(\nu)<0$ when $\nu<\nu_0$ (see Fig 5). We discuss measuring homeomorphism defects and easier to compute suitable surrogates in Sec. V.

As a short explanation for the gaps, we note that since

$$h_T(T_\nu) < h_T(T_{\nu_0}) = h_T(S_{a,b}), \tag{20}$$

the only way that we match equivalent orbits under the T and S dynamics is to restrict the domain of S. In other words, there must be orbits of S that cannot be represented by T, and the "gaps" indicate those initial conditions in S whose trajectories do not have a matching trajectory under T.

In the case $\nu>\nu_0$, the entropy mismatch is in the other direction, with

$$h_T(T_\nu) > h_T(T_{\nu_0}) = h_T(S). \tag{21}$$

There are now orbits in T that cannot be represented in S. Consequently, the commuting function f_ν must "remove" an appropriate amount of entropy from the T dynamics by mapping multiple points in the domain to single points in the range, so f_ν is not 1-1. Numerically, we observe similar discontinuities at $x=1/2$ (repeated in accordance with the kneading sequence). We use the same measuring function $\hat{\lambda}(\nu)$ as defined in Eq. (19), but we note that $\hat{\lambda}(\nu)>0$ when $\nu>\nu_0$.

Despite any limitations of numerical approximations of $\hat{\lambda}(\nu)$, we know analytically that

$$\hat{\lambda}(\nu_0) = 0. \tag{22}$$

Consequently, we can apply typical scalar root finding algorithms (bisection, or secant algorithms, for example) to approximate ν_0.

III. CONSTRUCTING THE CONTRACTION MAPPING FOR GENERAL TRANSFORMATIONS

In this section, we consider more general classes of dynamical systems than the tent maps examined in Sec. II A. Our goal is to develop a methodology that will allow us to "solve" the commutative diagram. Our primary tool will be the construction of an appropriate operator whose fixed point yields a solution to the commutative diagram. We call this operator the *commutation operator.* Our approach to defining the operator will be to generalize the technique of Sec. II A, which constructed a contraction operator to solve the appropriate functional equation. We explain our method in two parts, first by showing the construction process when the dynamical systems are conjugate, and then we show how to adapt that method to the case in which the maps are not conjugate. For this general case, we do not prove that the commutation operator is a contraction, but on all numerical examples we have tested, it has converged to an approximate solution.

A. Constructing the commutation operator for conjugate maps

Here we must solve the commuting Eq. (1), $f\circ g_1=g_2\circ f$, for a general one-dimensional g_1 and g_2. To phrase this equation as a fixed-point problem, we would like to solve for f on the right-hand side, but because we are interested in the case in which g_2 generates chaotic dynamics, it will not be invertible. As we did with the tent maps, we tackle this problem by providing a piecewise definition for the operator, where on each piece we use a restricted subset of Y to define the g_2^{-1}. Note that an extended version of g_2^{-1} must be defined, which we will call $\hat{g}_2^{-1}$ in order to well define the contraction.

In this subsection, we assume that g_1 and g_2 are conjugate. Therefore, there is a homeomorphism h that satisfies the commutative diagram, and this h is called a conjugacy. It

is our goal to have h be a fixed point of our constructed operator. We demand that h map monotone segments of the graph of g_1 onto monotone segments of g_2. To simplify the explanation, we assume that X and Y are compact intervals. Let $\boldsymbol{x}=\{x_0,x_1,\ldots,x_n\}$, with $X\equiv[x_0,x_n]$, and g_1 monotone on each interval $[x_{i-1},x_i]$, for $i=1,\ldots,n$. This notation results in a natural decomposition of X into a union of disjoint subintervals,

$$I_{X1}=[x_0,x_1], \tag{23}$$

$$I_{Xi}=(x_{i-1},x_i], \quad i=2,\ldots,n, \tag{24}$$

$$X=\bigcup_i I_{Xi}, \tag{25}$$

where we have (arbitrarily) chosen the closure conditions of the intervals. Because of the conjugacy of the dynamical systems, there must exist $\boldsymbol{y}=\{y_0,\ldots,y_n\}$, with $Y\equiv[y_0,y_n]$ and g_2 monotone on each interval $[y_{i-1},y_i]$, with a similar decomposition of Y into a union of disjoint subintervals I_{Yi}.[23] To allow for well defined inverse functions, we denote

$$g_{2i}=g_2|_{I_{Yi}}. \tag{26}$$

Because f is a conjugacy, it must map monotone intervals of X to monotone intervals of Y, such that we may write

$$f[I_{Xi}]=I_{Yi}, \quad i=1,\ldots,n, \tag{27}$$

by which we infer the identity

$$f[I_{Xi}]=g_{2i}^{-1}\circ g_2\circ f[I_{Xi}]. \tag{28}$$

We can now rewrite the commuting equation (1) as a system of equations,

$$g_{2i}^{-1}\circ f\circ g_1[I_{Xi}]=f[I_{Xi}], i=1,\ldots,n. \tag{29}$$

Having now solved for f on the right-hand side (RHS) of Eq. (29), we can use this formulation to construct the commutation operator. Let $\mathcal{F}$ be the set of functions from X to Y. Then we define the operator $\mathfrak{C}_{g_1}^{g_2}:\mathcal{F}\to\mathcal{F}$, which takes $F\in\mathcal{F}$ to $\mathfrak{C}_{g_1}^{g_2}F$ by

$$\mathfrak{C}_{g_1}^{g_2}F(x)=\hat{g}_{2i}^{-1}\circ F\circ g_1(x)x\in I_{Xi}. \tag{30}$$

Note the slight change in notation between Eqs. (29) and (30) in that we now use $\hat{g}_{2i}^{-1}$ instead of simply g_{2i}^{-1}, where we still need to define and explain the former. We remark that g_{2i}^{-1} is defined only for the interval $g_2[I_{Yi}]$, which may not be all of Y. However, $F\circ g_1(x)$ may be any value in Y. Consequently, we need to extend g_{2i}^{-1} to all of Y. We define $\hat{g}_{2i}^{-1}$ such that it satisfies the following:

- $\hat{g}_{2i}^{-1}$ is continuous on Y.
- $\hat{g}_{2i}^{-1}\equiv g_{2i}^{-1}$ on $g_2[I_{Yi}]$.
- $\hat{g}_{2i}^{-1}$ is Lipshitz continuous on $Y-g_2[I_{Yi}]$, with Lipshitz constant $L<1$.

Simply by expanding the domain of definition for each of the inverses, we ensure that for each $x\in X$, $\mathfrak{C}_{g_1}^{g_2}F(x)$ exists, so that the commutation operator is well defined. The requirement on the Lipschitz constant is meant to increase the likelihood that the operator may be a contraction. However, the requirements, as stated, do not uniquely define $\hat{g}_{2i}^{-1}$. We have chosen to retain this flexibility because we find that a judicious choice of extension may ease the numerical implementation and provide additional insight into the relationship between the systems. In this paper, the examples have used one or the other of the following strategies: (i) assume $\hat{g}_{2i}^{-1}$ is constant on $Y-g_2[I_{Yi}]$, or (ii) when g_2 is piecewise linear, then simply assume that $\hat{g}_{2i}^{-1}$ lies on the same line as g_{2i}^{-1}.

Proposition 1. *Let g_1 and g_2 be conjugate, with $h:X\to Y$ the conjugacy. Then h is a fixed point of the* commutation operator, $\mathfrak{C}_{g_1}^{g_2}$.

Proof. Take an arbitrary x. Then there is an i such that $x\in I_{Xi}$. Because h is a conjugacy, it must map monotone intervals to monotone intervals. In particular, $h[I_{Xi}]=I_{Yi}$, which implies that $y:=h(x)\in I_{Yi}$. We apply the definition of the commutation operator,

$$\mathfrak{C}_{g_1}^{g_2}h(x)=\hat{g}_{2i}^{-1}\circ h\circ g_1(x). \tag{31}$$

Because h is the conjugacy, we know that $h\circ g_1=g_2\circ h$. Substituting into the above equation gives

$$\mathfrak{C}_{g_1}^{g_2}h(x)=\hat{g}_{2i}^{-1}\circ g_2\circ h(x)=(\hat{g}_{2i}^{-1}\circ g_2)(y). \tag{32}$$

Because $y\in I_{Yi}$ and $(\hat{g}_{2i}^{-1}\circ g_2)|I_{Yi}$ is equivalent to the identity, we have

$$\mathfrak{C}_{g_1}^{g_2}h(x)=y=h(x). \tag{33}$$

□

Although h is a fixed point of the operator, we have not established that we can use an iterative scheme to find h. In the best situation, we would like the commutation operator to be a contraction (as it was for the class of tent maps considered in Sec. II A). In application to maps with chaotic attractors, we have found that iteration under the operator numerically converges to a fixed-point function.

B. The *commutation operator* for maps that are not (necessarily) conjugate

We now consider the problem of creating a commutation operator when map g_1 and g_2 are not necessarily conjugate. We would like this operator to be a contraction, so that its fixed point could be found by fixed-point iteration. Moreover, we want the fixed point to satisfy the commutative diagram. In this section, we will simply address the problem of creating the operator such that the fixed point of the operator satisfies the commutation diagram on some positive measure subset. The primary difference between this problem and that of the preceding section is that because the systems are not conjugate, there is no *a priori* reason that we should be able to match monotonic intervals of one dynamical system to monotonic intervals of the other. Consequently, the method requires some *ad hoc* component that specifies this matching. As in the preceding section, the underlying principle is that we will construct an operator whose fixed point satisfies the commutative diagram. If the resultant operator is a contraction, then the fixed point can be found by an iterative method. In general, g_1 and g_2 are not conjugate, which means that the fixed point is not a conjugacy. We will use *commuter* to denote a fixed point of this general commu-

tation operator, where the term appropriately describes that the fixed point satisfies the commutative diagram.

To motivate our methodology, we start with the "idea" that the commuter, $f:X\to Y$ should act like a change of variables, associating a trajectory of dynamical system g_1 with a trajectory of g_2. In mapping an *interval* $I_x\subset X$ to a $f[I_x]\subset Y$, we would really like to be able to associate trajectories of points in I_x to trajectories of points in $f[I_x]$. If the systems are not conjugate, then the "matching" will not be perfect. When the two systems *are* conjugate, the commuter is continuous, mapping intervals to intervals, and we are able to easily identify an appropriate matching by the maximum intervals on which the dynamical systems are monotone. In essence, it is this matching that prescribes the operator.

Construction of the commutation operator requires that the mathematician, now acting as a modeler, make some choices regarding the particular matching scheme to be employed. To describe our technique, we will decompose the problem into two components: first, we define a set of *minimal requirements* to constructing the operator; secondly, we define a set of *recommended choices* for the construction, where we provide some justification for those recommendations.

The following are requirements for construction of a commutation operator:

1. Choose an integer n, which will be the number of intervals for which we will prescribe a matching.
2. Choose a collection of disjoint subintervals $\{I_{Xi}\}_{i=1}^{n}$, where $I_{Xi}\subset X$, and $I=\cup_i I_{Xi}$ is a closed set that is forward invariant under g_1. Without loss of generality, we assume that these intervals are ordered, such that if $x_1\in I_{Xi}$ and $x_2\in I_{Xj}$, then $x_1<x_2$ whenever $i<j$.
3. For each $i\in\{1,\ldots,n\}$, assign an inverse function $\hat{g}_{2i}^{-1}:Y\to Y$ which satisfies the following:
   - $\hat{g}_{2i}^{-1}$ is continuous on Y.
   - There is an associated interval $I_{Yi}\subset Y$, such that $\hat{g}_{2i}^{-1}$ acts like an inverse to g_2 on the interval I_{Yi}. Equivalently, for all $y\in I_{Yi}, \hat{g}_{2i}^{-1}(g_2(y))=y$.
   - $\hat{g}_{2i}^{-1}$ is Lipshitz continuous on $Y-g_2[I_{Yi}]$, with Lipshitz constant $L<1$.

Using the above minimal choices, the definition of *commutation operator* given in Eq. (30) remains notationally correct. However, we need to recognize that the construction depended upon the actual choices for $\{I_{Xi}\}$ and $\{\hat{g}_{2i}^{-1}\}$, and we should formally treat them as parameters in describing how the operator acts on functions,

$$\mathfrak{C}_{g_1}^{g_2}F(x)\equiv\mathfrak{C}_{g_1}^{g_2}(\{I_{Xi}\},\{\hat{g}_{2i}^{-1}\})F(x):=\hat{g}_{2i}^{-1}\circ F\circ g_1(x),\quad x\in I_{Xi}. \tag{34}$$

Based on our experience, we provide the following list of *recommendations* for formulating the commutation operator, where our goal is to improve the utility of the resultant fixed point. In particular, if the systems are conjugate, we would like the fixed point to be the required conjugacy. When the systems are not conjugate, we still would like it to act as a commuter from X to Y, while retaining as much of the character of a homeomorphism as possible. We recognize that in some modeling situations there will be good reasons to take alternative approaches to those outlined below.

- *Choose n to be as small as practical.* As n increases, the modeler is required to make more choices regarding which intervals of X should be matched with which intervals of Y. Unless the modeler has an *a priori* reason to force a particular matching, it is better to allow the algorithm to find a matching. Consequently, it is generally counterproductive to choose n to be larger than n_2, where n_2 is the number of monotone sequences of g_2. On the other hand, g_2 must be monotone on each interval I_{Yi} to allow the inverse to be defined. So if the graphs of $\hat{g}_{2i}^{-1}$ are to cover[24] the graph of g_2, we will need at least n_2 different inverse functions, requiring $n\geqslant n_2$. Therefore, we typically choose $n=n_2$.
- We usually require $I\equiv X$. As a slight weakening of that condition, we might simply require that I be a closed interval in X. The basic idea is that we would like the commuter to map X to Y, so we need to cover as much of X as is possible.
- If $n\geqslant n_2$, we will construct $\hat{g}_{2i}^{-1}$ so that I_{Yi} are disjoint and that $\cup_i I_{Yi}$ is a closed interval. Typically, $\cup_i I_{Yi}\equiv Y$. This construction allows the covering of g_2 described above. Additionally, because the I_{Xi} have been ordered, we assume that $\hat{g}_{2i}^{-1}$ have been chosen to reflect a similar ordering on the I_{Yi}.

Remark: For the divergence measurements of the commutator f discussed in the next section, we would like to have at least existence and uniqueness of f in all of the general settings just discussed. Our experience indicates that a useful f does exist uniquely for all of the widely varied modeling choices of domains, partitions, and nonconjugate systems we have made. For the time being, however, the generality of our method remains unproven, although our remarks are suggestive of how the methods of proof designed for specific examples may generalize. Observe that the expansiveness of g_2 is needed to give the contraction of g_2^{-1} and consequently its extension $\hat{g}_2^{-1}$ to prove a contraction mapping converging to f as shown in Lemmas 1–3.

IV. MEASURE OF MOSTLY CONJUGATE

Suppose we have two dynamical systems,

$$g_1:X\to X,\quad g_2:Y\to Y. \tag{35}$$

When the two systems are topologically conjugate, then the dynamics of one system completely describe the dynamics of the other. However, if they are not conjugate, we may find that "some" of the dynamics of one system can be described by the other. We might heuristically judge that "most" of the dynamics are well represented by the other system. In some sense, we could consider the two systems to be "close," but that description is only reasonable if we can describe a "distance from conjugacy." As an application, we consider this prototypical problem: Fix g_1, and consider some family $\mathcal{D}$ of dynamical systems; find the element $g^*\in\mathcal{D}$ that most closely approximates the *dynamics* of g_1. Topological conjugacy defines two systems as having the same dynamics, and

any notion of "distance to conjugacy" ought to provide a means of determining the extent to which the dynamics are similar. *In this section, we propose a construct that allows such a measurement.*

In Sec. III, we described a technique for finding a *commuter*, f, from g_1 to g_2. Although f satisfies the commutative diagram, it need not be a homeomorphism (and, therefore, not a conjugacy). Let $\lambda(f)$ be a measure of how far f deviates from a homeomorphism, with $\lambda(f)\equiv 0$ when g_1 and g_2 are conjugate. In Sec. V, we give a more thorough description of λ, but for now, we simply state that the measuring function λ should be defined with sufficient flexibility to measure f relative to the "important" subset of X and Y, where "important" and the associated measure would be problem-dependent and according to the modeler's choice of what to compare. If we define $\mathcal{CF}(g_1,g_2)$ to be the set of all commuters from g_1 to g_2, then for a given λ, we can define

$$\delta(g_1,g_2) \equiv \inf_{f\in(g_1,g_2)} \lambda(f). \tag{36}$$

As an expository description of δ, we may think of a commuting function f as taking us from dynamical system g_1 to g_2, and $\lambda(f)$ measures a cost. Then δ would describe a greatest lower bound for that cost. In general, we would not require that the cost function be symmetric,[25] so that $\delta(g_1,g_2)$ need not be the same as $\delta(g_2,g_1)$. However, we will require that $\delta=0$ if g_1 and g_2 are conjugate.

Although δ appears to be a useful *theoretical* construct, we have no method for performing the optimization to evaluate. Therefore, we also define a less global definition by taking the following approach: In Sec. III, we described techniques to construct the *commutation operator*, $\mathfrak{C}$, for a given g_1 and g_2. Suppose that within a certain class of problems, we choose a particular canonical technique to construct the commutation operator such that given a particular choice of g_1 and g_2, the operator is *uniquely* defined. This unique choice of operator will have an associated fixed point, $f_{\mathfrak{C}}$, which is a commuter. Then we can use this commuter to evaluate the cost of transforming between the dynamical systems, defining

$$d(g_1,g_2) \equiv \lambda(f_{\mathfrak{C}}). \tag{37}$$

In practical application, given a dynamical system g, we may wish to restrict the comparison to dynamical systems $\tilde{g}$ from a particular family $\mathcal{G}$. Some examples of such restricted families include the following:

- skew tents
- symmetric tents
- constant slope maps
- polynomial maps of degree n.

The point of using these restricted families is that (i) it may be easier to provide a methodology for producing *unique* commutation operators; (ii) we may choose families that are described by a finite set of free parameters, making it easier to search within that family; (iii) the properties of the canonical system may be universally understood. When applying this restriction to the general problem of comparing an arbitrary g_1 and g_2, it is then necessary to project the problem onto the family $\mathcal{G}$. We denote $\bar{g}$, the projection of g into $\mathcal{G}$, by

$$\bar{g} = \arg\min_{\tilde{g}\in\mathcal{G}} d(g,\tilde{g}). \tag{38}$$

From a theoretical aspect, we need to be concerned with both the existence and uniqueness of this minimizer. In this paper, we will simply argue that our approach is meant to give a computable approximation, and within that framework of numerical implementation, it appears that our projection operation is sufficiently robust. Using this projection, we now define a new measurement function $D_{\mathcal{G}}$ by

$$D_{\mathcal{G}}(g_1,g_2) = d(g_1,\overline{g_1}) + d(\overline{g_1},\overline{g_2}) + d(g_2,\overline{g_2}). \tag{39}$$

We make the following remarks regarding $D_{\mathcal{G}}$:

- If $g_1\in\mathcal{G}$, then we may choose $\overline{g_1}=g_1 \Rightarrow d(g_1,\overline{g_1})=0$.
- If $g_2\in\mathcal{G}$, then we may choose $\overline{g_2}=g_2 \Rightarrow d(g_2,\overline{g_2})=0$.
- If $g_1,\ g_2\in\mathcal{G}$, then $D_{\mathcal{G}}(g_1,g_2)\equiv d(g_1,g_2)$.
- If $\mathcal{G}$ is a sufficiently large family such that g_1 and g_2 can be (arbitrarily) well approximated, then we may expect

$$d(g_1,\overline{g_1}) = O(\epsilon), d(g_2,\overline{g_2}) = O(\epsilon)$$

and

$$D_{\mathcal{G}}(g_1,g_2) = d(\overline{g_1},\overline{g_1}) + O(\epsilon). \tag{40}$$

We also recognize that an alternative approach in choosing projections $\overline{g_1}$ and $\overline{g_2}$ would be to choose a projection pair that minimizes the sum, $d(g_1,g_1)+d(\overline{g_1},\overline{g_2})+d(g_2,\overline{g_2})$. However, that approach might add significant computational complexity to the optimization problem, and we have found the simpler approach to be sufficient in application.

A. Manifesto for our particular choice for $\mathcal{G}$

Consider the family of dynamical systems $\mathcal{T}$ defined as follows:

- Each $f\in\mathcal{T}$ is continuous and piecewise linear on $[a,b]$.
- For each $f\in\mathcal{T}$, $|T'(x)|=c$, constant wherever the derivative exists.
- For each $f\in\mathcal{T}$, $|T'(x)|$ exists for all but perhaps a finite set of points.

We call $\mathcal{T}$ the *the set of constant slope maps.* In several applications, we note that choosing $\mathcal{G}\subset\mathcal{T}$ results in some nice properties for the projections because they inherit these properties from dynamical systems characteristics of constant slope maps.

V. MEASURING THE DEVIATION FROM HOMEOMORPHISM

Suppose we have two dynamical systems, $g_1:X\to X$ and $g_2:Y\to Y$. Additionally, suppose $f:D\to R$ is a commuter, $f\circ g_1=g_2\circ f$. If f were a homeomorphism, then g_1 and g_2 would be conjugate. However, if we know that the two dynamical systems are not conjugate, then f must fail to be a homeomorphism. We desire to build a metric that measures the extent to which f fails to be a conjugacy. Our general strategy will be to define a *homeomorphic defect*, which pro-

vides a weighted average based on measurements of each possible failure. We denote

$\lambda_O(f)$={amount that f is not onto},
$\lambda_{1\text{-}1}(f)$={amount that f is not 1-1},
$\lambda_C(f)$={amount that f is not continuous},
$\lambda_{C^{-1}}(f)$={amount that f^{-1} is not continuous},

where we note that f^{-1} may not be well defined. While there are certainly many ways to define each of these components, a specific definition scheme should satisfy the following:

- $\lambda_O(f) \geqslant 0$, with equality when f is onto.[26]
- $\lambda_{1\text{-}1}(f) \geqslant 0$, with equality when f is 1-1.
- $\lambda_C(f) \geqslant 0$, with equality when f is continuous.
- $\lambda_{C^{-1}}(f) \geqslant 0$, with equality when f^{-1} is continuous.

We define *homeomorphic defect of f*, denoted $\lambda(f)$, as a convex combination

$$\lambda(f) = \alpha_1\lambda_O(f) + \alpha_2\lambda_{1\text{-}1}(f) + \alpha_3\lambda_C(f) + \alpha_4\lambda_{C^{-1}}(f), \quad (41)$$

where the weights satisfy

$$0 \leqslant \alpha_i \leqslant 1, \quad \text{and} \quad \sum \alpha_i = 1. \quad (42)$$

Our decision not to specify a particular choice for the weights allows the flexibility to "tune" this metric for a particular application. Then

$$\lambda(f) \geqslant 0, \text{ with equality when } f \text{ is a homeomorphism.} \quad (43)$$

We note that if the converse were to hold (such that 0 defect implied homeomorphism), then λ could be used to provide a "distance from conjugacy" for the two dynamical systems g_1 and g_2. In this paper, our primary goal is to maintain the flexibility of the definitions (to allow broader applicability). Indeed, to retain this flexibility, our definitions are measure-based and, consequently, we expect that the converse will not hold.

A. Supporting assumptions and notation

We assume measure space/s $(D_1, \mathcal{A}_1, \mu_1)$ and $(D_2, \mathcal{A}_2, \mu_2)$, where $D_1 \subset X$ and $D_2 \subset Y$, $\mathcal{A}_1$ and $\mathcal{A}_2$ are σ algebras and μ_1 and μ_2 are measures. D_1 and D_2 are "chosen" by the modeler, and represent the subsets of X and Y that are of interest to the modeler. For example, one might be interested in comparing the dynamics of g_1 and g_2 on their forward invariant sets, which might be smaller than the whole space of the dynamics. Additionally, by allowing the modeler to *specify* a measure, the "important" parts of the sets D_1 and D_2 can be more heavily weighted. In some cases, the dynamics of interest might lie on $D_1 = C$, with C an invariant Cantor set with Lebesgue measure-0. We may still choose μ_1 such that $\mu_1(D_1) > 0$, which would allow us to measure subsets of D_1 in ways that will distinguish there size. Typically, we will be interested in chaotic dynamics, and assume that X and Y are bounded sets. In all the examples in this paper, the sets D_1 and D_2 are closed intervals and μ_1 and μ_2 are Lebesgue measures; for simplicity, we call this the *standard case*. Unless otherwise stated, we assume that μ_1 and μ_2 are *finite* and *nonatomic* measures. Additionally, we assume that $D_1 \subset \mathbb{R}^n$ and $D_2 \subset \mathbb{R}^n$, with topologies inherited from the usual topology. Our notation is that $f: D \to R$ is a commutator. Generally, we think of D_1 as being a restriction to a set of interest, but we do not preclude the case that $D_1 \subset D$ (or similarly $D_2 \subset R$). These situations reflect that sometimes the modeler is interested in a set that is larger than where the commutator is defined. As necessary, we will simply assume that the subsets resulting from various intersections are μ_1 or μ_2 measurable whenever this measurability is required by some definition. For ease of notation, we define

$$\overline{\mu_2}(f[A]) = \mu_2(f[A \cap D_1] \cap D_2) \quad (44)$$

for arbitrary set $A \subset X$. The idea is that we want to restrict ourselves to measuring image points that lie in D_2, whose pre-image was in D_1. Similarly, we define

$$\overline{\mu_1}(f^{-1}[B]) = \mu_1(f^{-1}[B \cap D_2] \cap D_1). \quad (45)$$

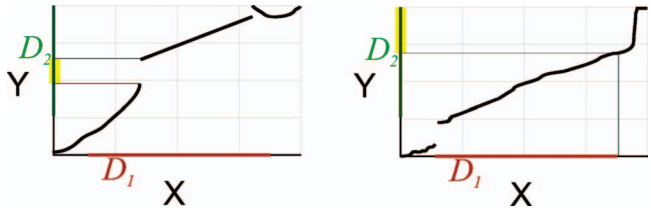

FIG. 6. (Color) Illustration of onto deficiency. See the definition of λ_O, Eq. (46). The space X is represented on the horizontal, with Y the vertical. The sets of interest, D_1 and D_2, are colored red and green. On each graph, we show an example of the graph of a commuter, $f(x)$. The "onto-deficiency" is computed from a μ_2 measure of the yellow portion. The right-hand example illustrates that (1) we are only interested in measuring the extent to which D_2 is covered (so the lower gap is not a problem), and (2) we are only allowed to use the part of f that is over D_1.

B. "Onto" deficiency

To measure the onto deficiency, we desire to measure the fraction of D_2 which is not covered by the range of f. We define the onto deficiency, λ_O, of the function f by

$$\lambda_O(f) = 1 - \frac{\overline{\mu_2}(f[D_1])}{\mu_2(D_2)}. \quad (46)$$

See Fig. 6.

Because f may have fractal structure with the range of f a Cantor set, it may be difficult to implement Eq. (46) in computational practice. As a "suitable surrogate," we find that if D_2 is an interval and μ_2 is absolutely continuous, we can often quantify the lack of onto-ness by finding the "biggest hole" in the range of f. Specifically, if we define

$$G := D_2 - f[D_1], \quad (47)$$

then a suitable surrogate is given by

$$\tilde{\lambda}_O(f) := \sup_{I \subset G} m(I), \quad (48)$$

where I is an interval and m is a Lebesgue measure. Note that generally $\tilde{\lambda}_O(f) \approx \lambda_O(f)$, but we expect that the values $\tilde{\lambda}_O(f)$ and $\lambda_O(f)$ will both change in the same direction (either increase or decrease) in response to a change in the argument function f. In other words, the hallmarks of an

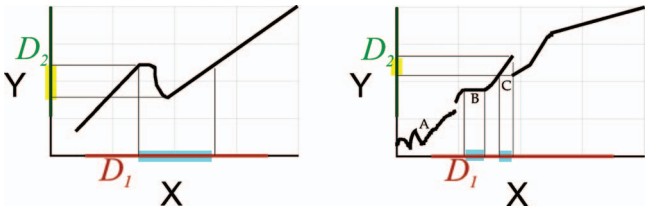

FIG. 7. (Color) 1-1 defect. See definition of $\lambda_{1\text{-}1}$, Eq. (49). (Left) A typical deficiency, where we take a μ_1 measure of the set that must be removed from D_1 to make the remaining function 1-1 (the blue horizontal segment) and a μ_2 measure of the portion of D_2 which is multiply covered (the yellow). (Right) In this example, note (1) the nonmonotonicity near region A is not measured, because it lies outside the sets of interest; (2) the horizontal component in region B results in a defect from the horizontal measurement, but no contribution from the vertical; (3) in region C, we take the interval to the left of the jump to perform the horizontal measurement because of the inf in the definition of $\lambda_{1\text{-}1}$.

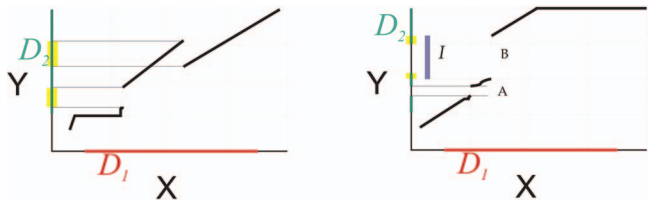

FIG. 8. (Color) Continuity defect. See definition of λ_C, Eq. (56). (Left) For a typical discontinuity, we μ_2 measure the size of the jump (and then choose the largest such jump). (Right) When D_2 is not an interval, we must be more careful. The discontinuity in region A does not create a defect, because it lies outside of D_2, while in region B, we only measure the portion of I that lies inside D_2.

appropriate *suitable surrogate* are such monotonicity with respect to parameter variations between $\tilde{\lambda}$ and λ. This may not always hold true, but it is often true in application on the simple examples we describe here.

C. 1-1 deficiency

To measure the extent to which f is not 1-1, we need to quantify *where* the function is not 1-1, by measurement on the domain of f, and the extent of the folding,[27] a measurement on the range. We proceed as follows: we define $\mathcal{G}$ to be the collection of all subsets $G \subset D_1$ which satisfy the following:

- G is μ_1 measurable.
- $f[G]$ is μ_2 measurable.
- f is restricted to G is 1-1.

For any such G, we denote its complement in D_1 by $\bar{G} \equiv D_1 - G$. Then we define the 1-1 *defect* by

$$\lambda_{1\text{-}1}(f) := \inf_{G \subset \mathcal{G}} \left[\frac{\mu_1(\bar{G})}{2\mu_1(D_1)} + \frac{\overline{\mu_2}(f[\bar{G}])}{2\mu_2(D_2)} \right]. \tag{49}$$

See Fig. 7.

In the *standard case,* we simply try to identify the largest part of the range that is multiply covered. We define envelope functions

$$e^+(x) = \sup_{D_1 \ni y \leqslant x} f(y), \tag{50}$$

$$e^-(x) = \inf_{D_1 \ni y \geqslant x} f(y). \tag{51}$$

Then $e^+(x)$ records the largest function value to the left of x, while $e^-(x)$ records the smallest function value to the right of x. Then

$$\tilde{\lambda}_{1\text{-}1}(f) = \|e^+(x) - e^-(x)\|_p. \tag{52}$$

We often choose $p=\infty$, yielding the sup norm, but other choices for p may be useful in some situations.

D. Measuring discontinuities of *f*

To measure discontinuities, we note that a continuous function maps "small sets to small sets," and that a discontinuity is indicated when an arbitrarily small set is mapped to a large one. In particular, we seek to identify when the f undergoes a "jump," and measure the jump. To allow the possibility of Cantor sets for D_1 and D_2, we will need to define these ideas in terms of sets and measures of those sets.

For each $x_0 \in D_1$ and for each $\delta > 0$, we define the set

$$\mathcal{B}(\delta, x_0) := \{x : x \in D_1, |x - x_0| < \delta\}, \tag{53}$$

which creates a nested family of sets as $\delta \searrow 0$. We measure the f image of these sets by defining

$$a_\delta(x_0) := \inf_{I \supset f[\mathcal{B}(\delta, x_0)]} \frac{\mu_2(I \cap D_2)}{\mu_2(D_2)}. \tag{54}$$

Because $a_\delta(x_0)$ is monotonically decreasing with decreasing δ, we can take the limit as $\delta \searrow 0$, defining

$$a(x_0) := \lim_{\delta \to 0^+} a_\delta(x_0), \tag{55}$$

where we think of $a(x_0)$ as being the *atomic* part of f.[28] We define

$$\lambda_C(f) := \sup_{x_0 \in D_1} a(x_0). \tag{56}$$

See Fig. 8.

Because $\lambda_C(f)$ is fundamentally based on intervals, we generally find that it is sufficiently easy to approximate such that we have not used a surrogate. However, we note that if D_1 is an interval, we can define

$$\tilde{\lambda}_C(f) = \|a(x_0)\|_p. \tag{57}$$

We note that $\tilde{\lambda}_C(f) \equiv \lambda_C(f)$ when $p=\infty$, but the flexibility to use other norms might prove useful in some situations.

E. Discontinuity in f^{-1}

In the *standard case*, we note that if f is 1-1 and continuous, then f^{-1} is well defined and is also continuous, so this requirement on a conjugacy may seem redundant. Generally, this requirement for a topological conjugacy is needed because the domain space and range space may be defined with very different topologies. In our situation, although the topologies are typically similar (based on inheriting the usual

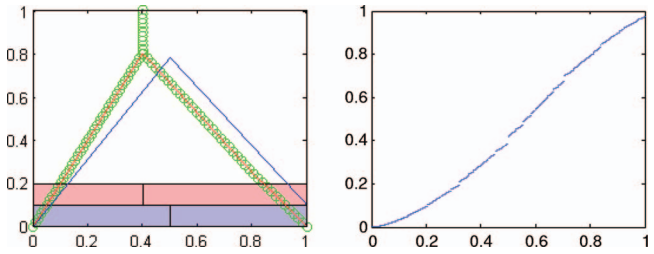

FIG. 9. (Color) These two tent maps are almost conjugate. $\tilde{\lambda}(f) \approx 1/4(0.032+0+0.032+0)$. Note that $g_1(1) \neq 0$.

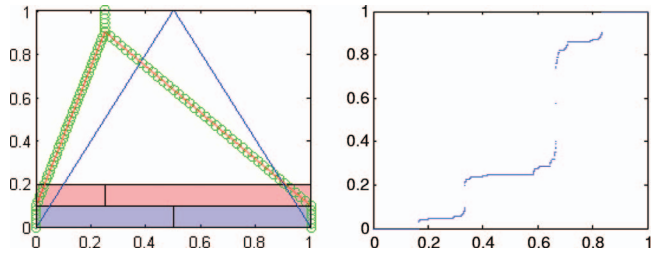

FIG. 10. (Color) Maps that are not close to conjugacy. $\tilde{\lambda}(f) \approx 1/4(0+0+0+0.163)$. Near $x=1/2$, the commuter, f is actually horizontal, indicating that there is an interval of orbits of g_1 than cannot be represented in g_2, but are instead associated with the vertical sections of the green graphs of g_2, which we defined as $\hat{g}_{2i}^{-1}$, which "complete" the inverse of g_2, as required by Eq. (30). The apparent vertical gap of the commuter is not a defect of continuity, but is simply the result of an extremely steep section in the graph, and not enough points are plotted to fill in the picture. We know there is no actual vertical gap because g_1 is a full shift and is able to match all orbits of g_2.

topology of the line), we find that directly measuring this fourth defect is the easiest and most direct way to measure gaps in the domain of definition. To define this defect, we employ the same strategy as for measuring the continuity of f.

For each $y_0 \in D_2$ and for each $\epsilon > 0$, we define the set

$$\mathcal{B}(\epsilon, y_0) := \{y : y \in D_2, |y - y_0| < \epsilon\}. \tag{58}$$

We measure the pre-image of these sets by defining

$$\hat{a}_\epsilon(y_0) := \inf_{I \supset f^{-1}[\mathcal{B}(\epsilon, y_0)]} \frac{\mu_1(I \cap D_1)}{\mu_1(D_1)}. \tag{59}$$

Taking the limit $\epsilon \searrow 0$, we define

$$\hat{a}(y_0) := \lim_{\epsilon \to 0} \hat{a}_\epsilon(y_0), \tag{60}$$

where we think of $\hat{a}(y_0)$ as being the *atomic* part of f^{-1}. We define

$$\lambda_{C^{-1}}(f) := \sup_{y_0 \in D_2} \hat{a}(y_0). \tag{61}$$

In the *standard case*, we use this defect to measure gaps in the domain. Similarly as for λ_C, a suitable surrogate is to measure the largest such gap in the domain. We define $\mathcal{I}$ to be the set of all intervals $I \subset D_1$ such that $f(x)$ is undefined or constant for all $x \in I$. Then we measure the defect as

$$\tilde{\lambda}_{C^{-1}}(f) = \sup_{I \subset \mathcal{I}} m(I), \tag{62}$$

where m is a Lebesgue measure.

The picture for $\lambda_{C^{-1}}(f)$ is not shown, but would be similar to that shown for $\lambda_C(f)$ in Fig. 8, where the roles of domain and range are reversed in the obvious manner for inverse functions.

VI. EXAMPLES

In this section, we present several examples of comparing maps g_1 and g_2 by showing the resulting commuter f, whether it be a homeomorphism or not (Figs. 9–16). Each example follows the same presentation template: in the left panel, we graph g_1 in blue and g_2 in red. Additionally, the graphs for $\hat{g}_{2i}^{-1}$ are displayed in green circles. Along the horizontal axis, the blue and red rectangles indicate the chosen intervals I_{Xi} and I_{Yi}. The right panel graphs the resultant commuter function created by repeated application of the commutation operator. For each commuter, the caption shows the approximate computation $\tilde{\lambda}(f) = 1/4(\tilde{\lambda}_O + \tilde{\lambda}_{1\text{-}1} + \tilde{\lambda}_C + \tilde{\lambda}_{C^{-1}})$.

VII. CONCLUSIONS

In this paper, we have put forward a generalizable method based on functional fixed-point iteration to explicitly construct the change of coordinates function that acts as a conjugacy between two topologically conjugate dynamical systems. We expect that our method of fixed-point iteration will extend, in a straightforward manner, to building conjugacy functions between higher dimensional systems when the symbol generating partitions are available. Of course, we know that this last caveat[29,30] is nontrivial, and this research is one aspect of our continuing work in the subject.

While construction of conjugacy functions is interesting in its own right, we do not consider this to be the main intellectual contribution of the work. In our opinion, a remarkable aspect of our methods of fixed-point iteration is that it still produces a commuter, even between nonequivalent systems, and in a sensible manner according to choices

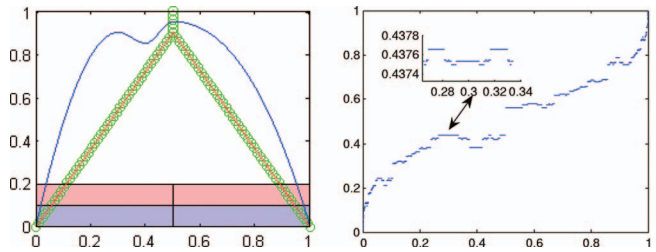

FIG. 11. (Color) Logistic map with "just a little" extra dynamics. Although these maps are nearly the same height, they are far from conjugacy. That g_1 has two humps, and g_2 has one hump, which suggests that subshifts of Σ_4 and Σ_2, respectively, are required to represent the dynamics. $\tilde{\lambda}(f) \approx 1/4(0.12+0.056+0.12+0)$. However, g_1 behaves as if it is almost conjugate to a trapezoid map (Ref. 37), also known as a gap-map (Ref. 38), since it does not take a large perturbation to replace the extra humps of $x \in (0.25, 0.5)$, with a horizontal line segment. However, our first choice, using a tent map of approximately the same height as g_1, does not match very well. Note the vertical gaps in the commuter, indicating that g_2 has dynamics that are not matched by g_1.

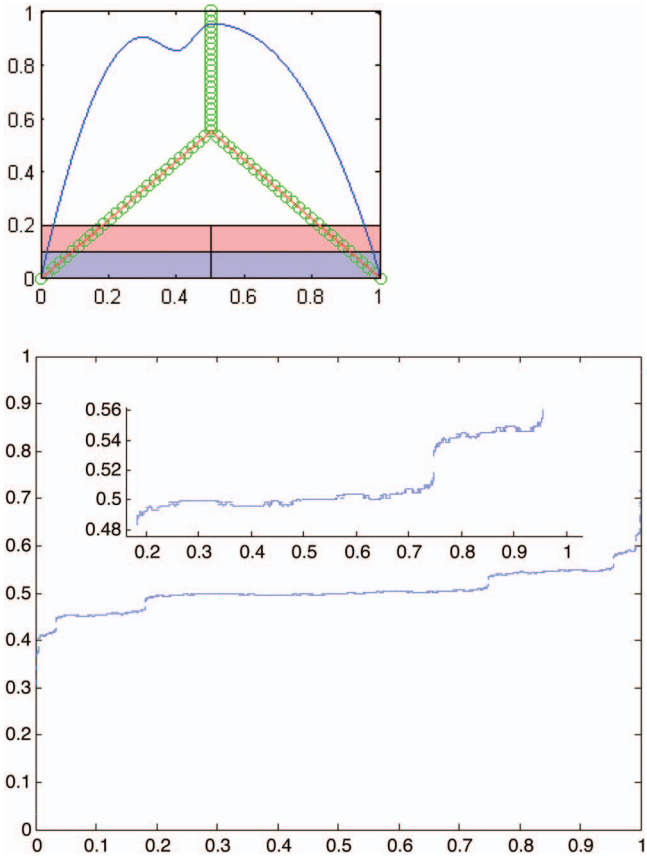

FIG. 12. (Color) Better projective comparison. The blue map g_1 is identical to that shown in Fig. 11, but here it is compared to a shorter tent map, $g_2(x)=T_{0.55}$. Therefore, this g_2 involves much less folding of the interval into itself than the g_2 of Fig. 11. Because of the L^1 difference between the maps, we might presume g_2 is less close to g_1 in an almost conjugacy sense. However, our almost conjugacy surrogates measure $\tilde{\lambda}(f)\approx 1/4(\epsilon_1+0.004+\epsilon_3+0.031)$, where ϵ_i denotes a numerically small value, which is significantly smaller than the defect in Fig. 11. Although the graph seems to indicate a large onto deficiency, the small $\tilde{\lambda}_O$ can be understood by first considering only the invariant sets of each map, $D_1=[0.201,0.95]$ and $D_2=[0.495,0.55]$, instead of the unit intervals [0, 1] shown. This scenario is emphasized by the inset picture of f, where we can see that $\tilde{\lambda}_O$ is small, and the other defects are even smaller. Comparing the maps g_1 and g_2 outside of the invariant sets, say on the left sides, near $x=0$, the maps are very similar: each sweeps initial conditions monotonically into D_1 and D_2, respectively. Thus the extension of f to the full [0, 1] to [0, 1] does not suffer the apparent onto deficiency near $x=0$ and $x=1$. $\tilde{\lambda}_{1\text{-}1}$ is small because this surrogate measures only the difference between the upper and lower envelope, as per Eq. (52). f is not continuous, but $\tilde{\lambda}_C$ is small since the vertical steps are short. The largest defect measurement, $\tilde{\lambda}_{C^{-1}}$, comes from short horizontal components, which are measured as discontinuities in f^{-1}. Why would the much shorter tent map g_2 here measure better as almost conjugate than the g_2 shown in Fig. 11? The result is reasonable when we focus on invariant sets: The blue curve on its invariant set is much more like the green g_2 in this example than the g_2 in Fig. 11, where a large fraction of the unit interval is folded over itself. We conclude that although the blue curve is tall, on its invariant set, it appears to be much like a scaled, almost conjugate, version of the short tent map on its invariant set.

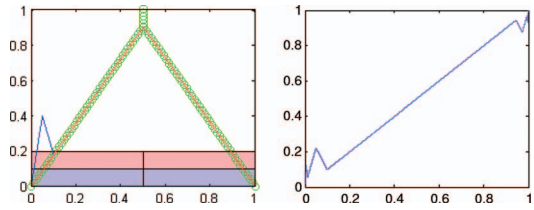

FIG. 13. (Color) Identical on the invariant set. For this example, g_1 and g_2 are identical on the interval [0.1, 1]. However, whereas g_2 is a simple tent map, g_1 has an additional hump on the interval [0, 0.1]. Because the maps are the same over a portion of the domain, the commuter coincides with the identify map on an interval. $\tilde{\lambda}(f)\approx 1/4(0+0.12+0+0)$. If dynamics were restricted to the invariant set of each system, then the two maps would be conjugate, with $f(x)=x$ the homeomorphism.

and preconceptions of the modeler. We put forward that the major contribution of this work is the thesis that dynamical systems should be comparable in a sense that is consistent with the topological conjugacy notion of equivalence; this is, after all, the centerpiece of the field of dynamical systems. Whereas nonequivalent systems have typically been compared by choice of a particular functional Banach space, such as L^2, it is obvious and well known that similarity or dissimilarity within such a norm does not directly address comparison between orbits of the two systems. Instead, we have claimed that comparison of nonequivalent dynamical systems could be made via the commuter function by measuring how it fails to be a homeomorphism. We believe that the specific details of our defect cost function λ are reasonable and useful to our stated purposes in the manifesto of Sec. IV A. Furthermore, we have designed flexibility for the modeler to design the details of λ so as to focus on various aspects of the mismatch. As we have shown in the examples of Sec. VI, a nonzero defect is generally descriptive of nonmatching between some of the orbits of the two dynamical systems, and the *concept* of measuring mismatch is the main issue we wish to emphasize, separate from the details of our defect functions. Thus, beyond entropy, we have outlined a new method measuring the dissimilarity of the languages corresponding to orbit structures of two nonequivalent dynamical systems. In this sense, our new methods may be considered more natural, within the context of a dynamical systems-based comparison, than a direct comparison of the right-hand sides of dynamical systems by using the norm of the difference in some Banach space.

There are a number of theoretical and applications oriented directions that we are currently pursuing in the future development of this work. These efforts include a topological based parameter estimation scheme for modeling dynamical systems within an assumed model classes, for example to match "toy models" to observed data. Similarly, our methods should be considered as a principled way to validate models produced by analysis of time-delay embedded data, where the primary desire is proper representation of the dynamical characteristics of the original system. Furthermore, since certain systems of differential equations (such as the Lorenz equations) admit Poincaré surface of sections which are very much like one-dimensional maps, our techniques are already directly applicable to such ODEs. We are also pursuing an extension of our fixed-point iteration scheme to allow for multivariate systems, within our ability to decide generating partitions. In this context, there is promise to extend our methods for comparison of general classes of differential equations. There is no fundamental roadblock to a multivariate extension of the fixed-point iteration scheme, and since

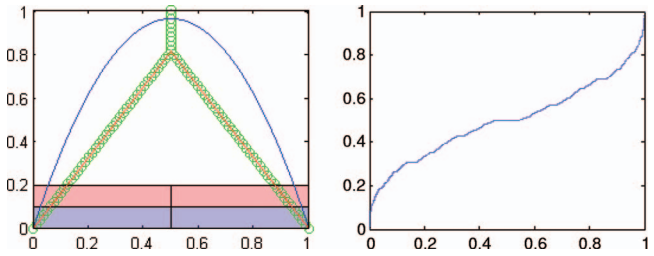

FIG. 14. (Color) The period–3 window. Choosing g_1 to be the logistic map with parameter 3.84, there is an attracting period–3 orbit whose basin is a point in the interval. A Cantor set of initial conditions that are not in that basin constitute a chaotic saddle of g_1. We compare this map to a submaximal tent map, where we have chosen the height of that tent map so that the defect will be small, with $\tilde{\lambda}(f) \approx 1/4(0.0005+0+0.0005+0.022)$. A higher tent map would create large intervals on which f is horizontal, while choosing a smaller tent would create larger vertical gaps. Each horizontal component indicates that f is associating an interval of g_1 dynamics to a single point in g_2.

the design of the defect functions was entirely measure-based, it will extend directly to this setting. A future goal for this work is to be able to measure the degree to which a toy model is descriptive of the larger system (such as a Galerkin projection of a PDE).[39,40]

ACKNOWLEDGMENTS

This research was supported under NSF Grant No. DMS-0404778. We thank the anonymous referees for their thorough feedback and thoughtful suggestions.

APPENDIX A: QUADWEBBING

"Quadwebbing" is our name for a graphical representation that allows us to visualize the action of the both commutation operator and the commuter in relation to one-dimensional (1D) maps of the interval. The basic structure of a quadweb diagram is based on the idea that we seek to

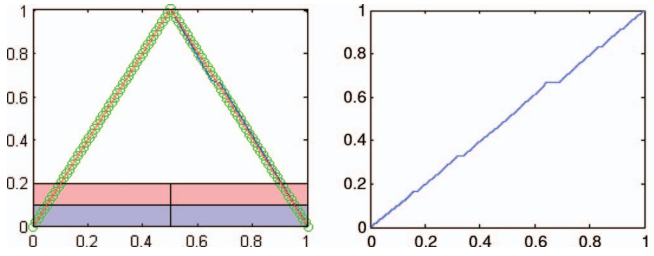

FIG. 15. (Color) Two full-shift maps that are not conjugate. g_1 is a slight alteration of the full-shift symmetric tent. The right leg has been modified so that a small portion has a slope m, with $|m|<1$, where that interval contains the fixed point. Therefore, g_1 has a stable fixed point at $x_f=0.665$. This commuter is similar in character to that of Fig. 14—the stable periodic point of the X dynamics means that an entire interval of initial conditions must be associated with a single point in the Y dynamics. Since the initial condition is in the basin of attraction for this fixed point, the resultant commuter is a devil's staircase function. $\tilde{\lambda}(f) \approx 1/4(0+0+0+0.048)$. We remark that when measuring the defect via suitable surrogate, the deficiency caused by horizontal portions of the commuter is recorded as a defect in the continuity of the inverse, not by the defect in 1-1.

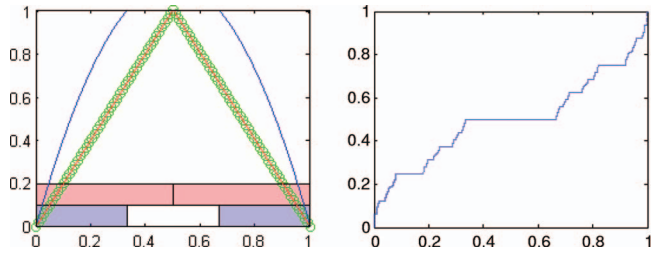

FIG. 16. (Color) The "too-tall" logistic map. The literature (Refs. 5 and 9) tells us that the invariant set of this logistic map is semiconjugate to the full tent map. This relationship is a conjugacy if the domain of the tent map excludes the peak point, and all of its pre-images. This commuter f, shown here for the first time, has defects $\tilde{\lambda}(f) \approx 1/4(0+0+0+1/3)$, and it is, in fact, a devil staircase function with flat spots over the holes of a Cantor set. Notice the strong similarity to the previous two examples.

understand the relationship between dynamical systems g_1 and g_2 within the context of the commutative diagram:

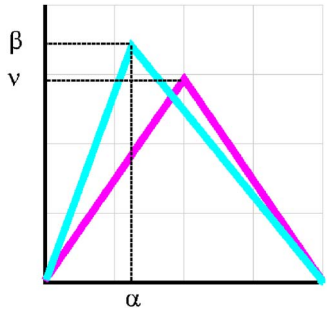

$$\begin{array}{ccc} X & \xrightarrow{g_1} & X \\ f\downarrow & & \downarrow f \\ Y & \xrightarrow{g_2} & Y \end{array} \tag{A1}$$

Each quadweb is constructed by dividing the figure into a two-by-two panel of axes, where each panel shows the graph of one of the four functions shown in the commutative diagram. The plots are arranged to allow a graphical illustration of how the function f satisfies the commutative diagram. Figure 1 (left) illustrates the case of conjugate dynamical systems.

In addition to illustrating how the commuter satisfies Eq. (A1), it reveals where it might fail. Specifically, as we recall from Sec. III, we noted that to have a well defined operator, we needed to extend the graph of g_2 such that its inverse could be applied to any $y \in Y$. We denoted the modified graphs as $\hat{g}_{2i}^{-1}$. We use the term[31]

The *zed* describes that portion of the graph of

$$\hat{g}_{2i}^{-1} \text{ that does not coincide with } g_2. \tag{A2}$$

If $f \circ g_1(x)$ lies on the zed, then Eq. (A1) does not hold for that x. This phenomenon can be interpreted to mean that g_1 has more dynamics than can be represented by g_2 under the assumed partitions. Figure 17 illustrate this behavior.

The quadweb diagram allows for easy understanding of what some typical defects imply about the dynamics of the system. In particular, wherever f is horizontal, we see an interval of initial conditions for system g_1 that must be rep-

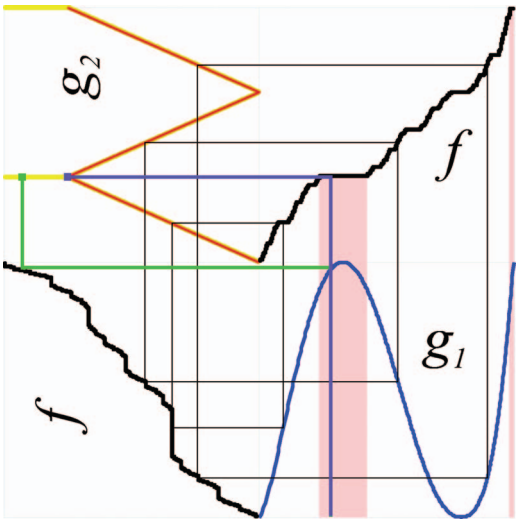

FIG. 17. (Color) Quadweb for nonconjugate maps. g_1 maps across X a full three times. g_2, shown in red, also has three laps, but they do not map completely across Y. The yellow graph shows the g_{2i}^{-1}, which are used to construct a well-defined commutation operator. The green path illustrates $f\circ g_1$ for a particular x. Using the same x, we use the purple path to show $g_2\circ f(x)$, which obviously does not coincide with the green. Rather the green path shows that we land on the *zed* which is the case for all x inside the intervals colored pink. The black rectangles illustrate that Eq. (A1) holds at x lying outside these intervals.

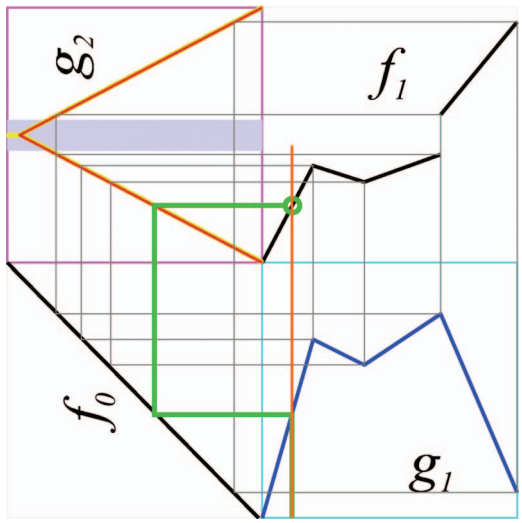

FIG. 18. (Color) Quadweb illustration of the commutation operator. For ease of illustration, we choose f_0 as the identify map, and plot it in the lower left corner. The orange vertical shows a chosen x coordinate, and the green path shows the graphical computation of $g_2^{-1}\circ f\circ g_1(x)$. The intersection in the upper right quad is a point that lies on $f_1=\mathfrak{C}_{g_1}^{g_2}f_0$. Generally, you would need to repeat for a large number of x coordinates. However, since all maps are linear in this example, a few well chosen points are sufficient to describe the first application of the commutation operator.

resented by a single point under g_2. Similarly [see Fig 1 (right)] when f has a vertical gap, there is an interval in g_2 that has no associated orbit in system g_1.

As a final illustration of alternative uses of the quadweb, we use the diagram to provide a graphical description of the action of the commutation operator. If we graph an arbitrary f_0 in the lower left panel, we can graphically compute $f_1=\mathfrak{C}_{g_1}^{g_2}f_0$ as follows: Choose an arbitrary x coordinate in the right half of the quadweb. Move up until you reach g_1, then left until you reach f_0, up again to g_2, then to the right. Although we used g_1 and f_0 in the usual way of graphically applying a function, we note that we used graph g_2 by going from range Y to domain Y, equivalent to applying g_2^{-1}. Consequently, we graphically "compute" the path $g_2^{-1}\circ f\circ g_1(x)$. The resultant intersection of that line with the original x coordinate is a point on f_1. Repeating at a sufficiently dense set of x coordinates will allow a robust description of f_1. See Fig. 18 for an example of this technique.

APPENDIX B: RELATIONSHIP TO DE RHAM FUNCTIONS AND LEBESGUE SINGULAR FUNCTIONS

In this appendix, we will give a direct and constructive proof of the singular nature of homeomorphisms between full shift tent maps. A standard result from ergodic theory gives that probability measures on distinct shift maps are mutually singular.[32] Since the conjugacy must map the uniform measure of the symmetric tent to the mutually singular probability measure on a skew tent, that conjugacy must be a singular function.[33] The purpose of including a proof of the special case form of this fact, in the form of Proposition 1 below, is that we hope that its constructive approach gives explicit intuition for general homeomorphisms, to the geometric constructive nature of the fixed-point iteration scheme highlighted in this paper, and some insight into what may become of the geometry of nonhomeomorphic commuters. We show that the conjugacy function $h(x)$ which results is both a Lebesgue singular function, and in many ways reminds us of a de Rham function. The similarity of our homeomorphisms $h(x)$ to the de Rham functions arises from the fact that both are solutions to functional equations of similar form. We note that required solutions to de Rham–like equations can arise quite naturally in other settings of dynamical systems,[34] with a standard solution approach of finding an expression of the problem that can be solved using the Contraction Mapping Principle.

We recall definitions of these peculiar functions before we proceed to prove the properties of our $h(x)$. While we have not proven that homeomorphisms between two tents that are not both full have these properties, and we also do not prove these properties for either nontent maps or nonfull shift tent maps, the properties are certainly suggestive of the nature of the kinds of peculiarities one might expect, and even which seem apparent in the simulations. Most striking is the degree to which we now know that the usual homeomorphism example between a full tent and the full logistic map, which gives rise to a diffeomorphism, can mislead intuition from the more typical conjugacy.

1. Lebesgue singular functions

Definition [36]: A continuous function of bounded variation $s(x)$ is called a *singular function* if it is differentiable almost everywhere on its domain, and the derivative $s'(x)=0$ where it exists, and it is called a *Lebesgue singular function* when almost every one is in the sense of a Lebesgue measure.

Definition [39 and 40]: *de Rham functions*. A de Rham

function is the unique bounded solution of the functional equation

$$\phi\left(\frac{t}{2}\right) = a\phi(t), \quad \phi\left(\frac{t+1}{2}\right) = a + (1-a)\phi(t), \tag{B1}$$

where $a \in (0,1)$ is fixed and Eq. (B1) is satisfied for all $t \in [0,1]$.

2. $h(x)$ is a singular function

In this section, we will show that for some parameter values, the f_ν that results from Lemma 3 is a singular function. The argument of this proof follows closely the structure found in Ref. 19, which is standard for the de Rham functions. However, slight modifications to the proof are required due to the differences between his problem and ours. We will specifically consider the conjugacy between a full shift skew tent map and the full shift symmetric tent.

Consider the set of skew tent maps of the form $S_{a,1}$, which are the maps that generate a full shift on two symbols. These maps are conjugate to the full shift symmetric map, T_1, by which we infer that $\nu=\nu_0=1$. If $a=1/2$, then $S \equiv T_1$, and the conjugacy would be the identify map. However, when $a \neq 1/2$, we can find the conjugacy h by developing the contraction operator and identifying its fixed point. Then $f_\nu \equiv f_{\nu_0} \equiv f_1 \equiv h$. Because h is a conjugacy, we know it is strictly increasing and continuous. However, we will find that despite these restrictions, h remains a very strange function.

Recall[35,36] that by the *Lebesgue Decomposition Theorem*, a function $g(x)$ of bounded variation may be decomposed,

$$g(x) \equiv a(x) + s(x), \tag{B2}$$

where $a(x)$ is absolutely continuous and $s(x)$ is purely singular. As an additional description of this decomposition, we have

$$a(x) = \int g'(x)\mathrm{d}x \Rightarrow g(x) = s(x) + \int g'(x)\mathrm{d}x. \tag{B3}$$

So the singular part separates out the components that prevent a function from satisfying the fundamental theorem of calculus. Because h is strictly monotone and continuous on a closed interval, it is of bounded variation, so it is decomposable as above. However, in the following paragraphs, we show that $h(x)$ is itself a purely singular function, such that

$$h(x) \equiv a(x) + s(x) \Rightarrow a(x) \equiv 0. \tag{B4}$$

Proposition 2. *Let $h(x)$ be the conjugacy between $S_{a,1} \in \mathcal{S}$ and T_1, where $a \neq 1/2$. Then $h'(x)$ exists for almost every $x \in [0,1]$. Moreover, $h'(x)=0$ wherever $h'(x)$ exists.*

Proof. Because h must be a homeomorphism, it is increasing. Then a standard result from analysis[36] tells us that h is a.e. differentiable, giving the existence of $h'(x)$. Suppose that the derivative exists at some $0<x<1$; we will show that $h'(x)=0$.

For each n, we find integer k_n such that

$$x \in I_n := \left(\frac{k_n}{2^n}, \frac{k_n+1}{2^n}\right]; \tag{B5}$$

measuring the range of h over the interval I_n, we define

$$p_n := h\left(\frac{k_n+1}{2^n}\right) - h\left(\frac{k_n}{2^n}\right). \tag{B6}$$

Since $h'(x)$ exists, we know that

$$h[(k_n)2^{-n},(k_n+1)2^{-n}] = \frac{p_n}{2^{-n}} \to h'(x), \tag{B7}$$

where the left-hand side symbolizes the Newton divided difference. If $h'(x) \neq 0$, then the ratio of two successive divided differences (for n and $n+1$) will tend to 1. Therefore, the ratio

$$\frac{p_{n+1}}{p_n} \to \frac{1}{2}, \tag{B8}$$

as long as $h'(x)$ is distinct from 0.

To complete the proof, we will show that either $p_{n+1}/p_n=a$ or $p_{n+1}/p_n=1-a$, where this property holds for all x. This portion of proof results from the self-similar structure that derives from the fact that $h(x)$ is the fixed point of the contraction mapping M_1 defined by Eq. (13), where we are using $b=\nu=\nu_0=1$. The proof proceeds by induction:

- **True for** $n=0$. We have $p_0=h(1)-h(0)=1-0=1$. If $x \leqslant 1/2$, then $I_1=(0,1/2]; h(1/2)=a$, and $p_1/p_0=a$. For $x > 1/2, p_1=h(1)-h(1/2)$, giving $p_1/p_0=1-a$.
- **Induction**. Assume that for arbitrary x, $p_{j+1}/p_j \in \{a,1-a\}$ for all $0 \leqslant j \leqslant n-1$. We will show that the property holds for $j=n$.

Note that the end points of I_n are $x_{\text{left}} := k_n/2^n$ and $x_{\text{right}} := k_n+1/2^n$. Denote the midpoint of I_n as x_{mid}. Then either $I_{n+1}=(x_{\text{left}},x_{\text{mid}}]$ (which implies that $k_{n+1}=2k_n$) or $I_{n+1}=(x_{\text{mid}},x_{\text{right}})$, implying $k_{n+1}=2k_n+2$. If we assume that I_{n+1} is on the left half of I_n, then

$$\frac{p_{n+1}}{p_n} = \frac{h\left(\frac{2k_n+1}{2^{n+1}}\right) - h\left(\frac{2k_n}{2^{n+1}}\right)}{h\left(\frac{k_n+1}{2^n}\right) - h\left(\frac{k_n}{2^n}\right)}, \tag{B9}$$

whereas if I_{n+1} is the right half of I_n, we have

$$\frac{p_{n+1}}{p_n} = \frac{h\left(\frac{2k_n+2}{2^{n+1}}\right) - h\left(\frac{2k_n+1}{2^{n+1}}\right)}{h\left(\frac{k_n+1}{2^n}\right) - h\left(\frac{k_n}{2^n}\right)}. \tag{B10}$$

We now take advantage of the self-similarity implied by Eq. (7): When $x \leqslant 1/2$, we have that $ah(2x)=h(x)$. So for each function evaluation in Eqs. (B9) and (B10), we perform the substitution

$$ah\left(\frac{m}{2^{r-1}}\right) = h\left(\frac{m}{2^r}\right). \tag{B11}$$

To simplify notation, we denote by I_n' the dyadic intervals containing the point $2x$, and define p_n' as the length of the

intervals $h[I'_n]$. Then applying Eq. (B11) to Eqs. (B9) and (B10), we have that

$$\frac{p_{n+1}}{p_n} = \frac{ah\left(\frac{2k_n+1}{2^n}\right) - ah\left(\frac{2k_n}{2^n}\right)}{ah\left(\frac{k_n+1}{2^{n-1}}\right) - ah\left(\frac{k_n}{2^{n-1}}\right)} = \frac{p'_n}{p'_{n-1}}, \tag{B12}$$

or

$$\frac{p_{n+1}}{p_n} = \frac{ah\left(\frac{2k_n+2}{2^n}\right) - ah\left(\frac{2k_n+1}{2^n}\right)}{ah\left(\frac{k_n+1}{2^{n-1}}\right) - ah\left(\frac{k_n}{2^{n-1}}\right)} = \frac{p'_n}{p'_{n-1}}. \tag{B13}$$

By assumption,

$$\frac{p'_n}{p'_{n-1}} \in \{a, 1-a\}. \tag{B14}$$

The argument for $x > 1/2$ is similar, though the scaling factor is $1-a$ instead of a. □

3. Remarks and lessons from the de Rham–like conjugacies

We have remarked that since two piecewise linear maps with different metric entropies must not be diffeomorphically related, then any conjugacy between two such maps cannot be everywhere differentiable. It may not be immediately obvious what is the distinguished point or points where the discontinuity of the derivative of $h(x)$ should reside. Now, in light of the analysis of the de Rham like properties of $h(x)$ in the previous section, we see that the discontinuities are dense, located at endpoints of the dyadic intervals I'_n, corresponding to preimages of the map peaks, where there is a discontinuity in the slope of the nth composition of the symmetric tent map.

[1] D. K. Arrowsmith and C. M. Place, *Dynamical Systems: Differential Equations, Maps and Chaotic Behavior* (Chapman & Hall, London,1992; G. L. Baker and J. P. Gollub, *Chaotic Dynamics* (Cambridge University Press, Cambridge, UK, 1990; R. L. Devaney, *An Introduction to Chaotic Dynamical Systems* (Benjamin/Cummings, Menlo Park, NJ, 1986); L. Glass and M. Mackey, *From Clocks to Chaos: The Rhythms of Life* (Princeton University Press, Princeton, 1988); I. C. Percival and D. Richard, *Introduction to Dynamics* (Cambridge University Press, Cambridge, UK, 1982); J. Pritchard, *The Chaos Cookbook: A Practical Programming Guide* (Butterworth-Heinemann, Oxford, 1992); S. Strogatz, *Nonlinear Dynamics and Chaos* (Addison-Wesley, Reading, MA, 1994).

[2] I. C. Percival, "Chaos: A Science for the Real World," New Scientist beginning with the October 21 issue, pages 20–25, continuing through the December 2 issue (1989).

[3] J. Gleick, *Chaos, the Making of a New Science* (Heinemann, London, 1987); I. Stewart, *Does God Play Dice?* (Blackwell, Cambridge, UK, 1989).

[4] H. Poincare, *Les Methods Nouvelles de la Mecanique Celeste* (Gauthier-Villars, Paris, 1892, 1893, and 1899), Vols. I, II, and III [*New Methods of Celestial Mechanics* (American Institute of Physics, New York, 1993)].

[5] Robert L. Daveney, *An Introduction to Chaotic Dynamical Systems*, 2nd ed. (Westview Press, Redwood City, California, 2003).

[6] J. Guckenheimer and P. Holmes, *Nonlinear Oscillations, Dynamical Systems, and Bifurcations of Vector Fields*, Applied Mathematical Sciences Vol. 42 (Springer, Berlin, 2002).

[7] B. P. Kitchens, *Symbolic Dynamics, One-sided, Two-sided and Countable State Markov Shifts* (Springer, New York, 1998).

[8] E. Ottt, *Chaos in Dynamical Systems*, 2nd ed. (Cambridge University Press, Cambridge, UK, 2002).

[9] C. Robinson, *Dynamical Systems; Stability, Symbolic Dynamics, and Chaos*, 2nd ed. (CRC Press, Boca Raton, FL, 1999).

[10] E. N. Lorenz, "A study of the predictability of a 28-variable atmospheric model," Tellus **17** 321 (1965).

[11] E. N. Lorenz and K. A. Emanuel, *Optimal Sites for Supplementary Weather Observations: Simulation with a Small Model* (American Meteorological Society, Washington, DC, 1998), p. 399.

[12] D. Lind and B. Marcus, *An Introduction to Symbolic Dynamics and Coding* (Cambridge University Press, New York, 1995).

[13] K. Thompsen, "The defect of factor maps and finite equivalence of dynamical systems," *Topics in Dynamics and Ergodic Theory*, edited by S. Bezuglyi and S. Kolyada (Cambridge University Press, Cambridge, UK, 2003), pp 190–225.

[14] L. Bunivmovich *et al.*, *Dynamical Systems, Ergodic Theory, and Applications*, 2nd ed., edited by Y. G. Sinai (Springer-Verlag, Berlin, 2000).

[15] G.-C. Yuan, J. A. Yorke, T. L. Carroll, E. Ott, and L. M. Pecora, "Testing whether two chaotic one dimensional processes are dynamically identical," Phys. Rev. Lett. **85**20, 4265 (2000).

[16] M. Shub, "Endomorphism of compact differentiable manifolds," Am. J. Math. **91**, 175 (1969).

[17] M. Shub and D. Sullivan, "Expanding endomorphisms of the circle revisited," Ergod. Theory Dyn. Syst. **5**, 285 (1985).

[18] W. de Melo and S. van Strien, *One-Dimensional Dynamics* (Springer-Verlag, Berlin, 1992).

[19] P. Billingsley, *Probability and Measure*, 3rd ed. (Wiley-Interscience, New York, 1995).

[20] M. Misiurewicz and E. Visinescu, "Kneading sequences of skew tent maps," Ann. I.H.P. Probab. Stat. **27**, 125 (1991).

[21] J. P. Eckmann and D. Ruelle, "Ergodic theory of chaos and strange attractors," Rev. Mod. Phys. **57**, 617 (1985).

[22] J. Hale, *Ordinary Differential Equations* (Kreiger, Melbourne, FL, 1980).

[23] The major step of choosing and matching partitions of the two dynamical systems is somewhat easier in one-dimensional phase spaces, with interesting and important consequences if for some reason the generating partitions are not matched, as studied in our previous work (Ref. 29). It may often be useful for complexity reduction of the models to deliberately not choose generating partitions, as exemplified by the examples in Figs. 11 and 12. In multivariate dynamical system, choosing the partitions to compare will be a challenging part of the problem in future work. For example, the generating partition for certain diffeomorphisms of the plane are conjectured to coincide to a curve connecting "primary" heteroclinic tangencies (Ref. 30) but again there is useful information to be gained by matching without regard to the generating partition (Ref. 29).

[24] *Cover*—with each $y \in Y$ we associate a point $(y, g_2(y)) \in Y \times Y$. The collection of all such points is called the *graph* of g_2. A point $(y, g_2(y))$ on that graph is covered by the inverse function $\hat{g}_{2i}^{-1}$ if there is a $p \in Y$ such that $(\hat{g}_{2i}^{-1}(p), p) \equiv (y, g_2(y))$.

[25] One may easily create a measuring definition that is symmetric, for instance, by defining $\bar{\delta} = \delta(g_1, g_2) + \delta(g_2, g_1)$.

[26] Ideally, we would want equality to imply the converse for each of these four statements (i.e., $\lambda_O = 0 \Rightarrow f$ is onto). However, because our approach to defining these defects is measure-based, the strongest condition we should expect is that we would satisfy these properties *almost everywhere*.

[27] By "folding," we mean to measure many-to-oneness, quantifying the amount of the range that has multiple pre-images.

[28] By *atomic part*, we mean to use the Lebesgue decomposition of a function (Ref. 36) into its continuous part and atomic part, $f(x) = c(x) + a(x)$. The theorem applies to functions of bounded variation, and sometimes f will not satisfy this hypothesis. However, since we do not require an actual decomposition, we view our verbiage as a minor abuse of notation. See Ref. 35 for a further discussion of this general decomposition.

[29] E. Bollt, T. Stanford, Y-C. Lai, and K. Zyczkowski, "What symbolic dynamics do we get with a misplaced partition? On the validity of threshold crossings analysis of chaotic time-Series," Physica D **154**, 259 (2001).

[30] P. Grassberger and H. Kantz, "Generating partitions for the dissipative Hénon map," Phys. Lett. **113A**, 235 (1985).

[31] Dr. Seuss, *One Fish, Two Fish, Red Fish, Blue Fish* (Random House, New York, 1960). [We recognize that literally the whole graph $\hat{g}_{2i}^{-1}$ would be a *zed*, with the portion extending beyond g_2 being the "hair" upon the head; we consider our definition to be only a minor abuse of notation.]

[32] P. Billingsley, *Ergodic Theory and Information* (Wiley, New York, 1965).

[33]W. Rudin, *Functional Analysis*, 2nd ed. (McGraw-Hill, New York, 1991), p. 121.
[34]S. Tasaki, T. Gilbert, and J. R. Dorfman, "An analytical construction of the SRB measures for Baker-type maps," Chaos **8**, 242 (1998).
[35]P. R. Halmos, *Measure Theory* (Van Nostrand, New York, 1950).
[36]A. N. Kolmogorov and S. V. Fomin, *Introductory Real Analysis* (Dover, New York, 1975).
[37]K. M. Brucks, M. Misiurewicz, and C. Tresser, "Monotonicity properties of family of trapezoidal maps," Commun. Math. Phys. **137**, 1 (1991).
[38]K. Zyczkowski and E. Bollt, "On the entropy devil's staircase in a family of gap-tent maps," Physica D **132**, 392 (1999).
[39]L. Berg and M. Krüppel, "de Rham's singular function and related functions," Z. Anal. ihre Anwend. **19**, 227 (2000).
[40]G. de Rham, "Sur quelques courbes définies par des équations fonctionelles," Rend. Semin. Mat. Torino **16**, 101 (1956).